

# Mechanism of carotenoid coloration in the brightly colored plumages of broadbills (Eurylaimidae)

Richard O. Prum · Amy M. LaFountain ·  
Christopher J. Berg · Michael J. Tauber ·  
Harry A. Frank

Received: 27 August 2013 / Revised: 3 February 2014 / Accepted: 12 February 2014 / Published online: 20 March 2014  
© Springer-Verlag Berlin Heidelberg 2014

**Abstract** The plumage carotenoids of six species from five genera of broadbills (Eurylaimidae) have been examined. These plumages are crimson, violet, purple-maroon, or yellow. Two genera also have brilliant green plumages that are produced by a combination of structural coloration and unknown carotenoids. Six different carotenoids from nine different plumage patches were identified, including two previously unknown molecules, using high-performance liquid chromatography, mass spectrometry, and MS/MS fragment analysis. The yellow pigment in *Eurylaimus javanicus* and *Eurylaimus ochromalus* is identified as the novel carotenoid, 7,8-dihydro-3'-dehydro-lutein.

Communicated by G. Heldmaier.

**Electronic supplementary material** The online version of this article (doi:10.1007/s00360-014-0816-1) contains supplementary material, which is available to authorized users.

R. O. Prum (✉)  
Department of Ecology and Evolutionary Biology and Peabody  
Museum of Natural History, Yale University, 21 Sachem Street,  
New Haven, CT 06511, USA  
e-mail: richard.prum@yale.edu

A. M. LaFountain · H. A. Frank  
Department of Chemistry, University of Connecticut, 55 North  
Eagleville Road, Storrs, CT 06269, USA  
e-mail: amy.lafountain@uconn.edu

H. A. Frank  
e-mail: harry.frank@uconn.edu

C. J. Berg · M. J. Tauber  
Department of Chemistry, University of California, San Diego,  
9500 Gilman Drive, La Jolla, CA 92093, USA  
e-mail: cberg@ucsd.edu

M. J. Tauber  
e-mail: mtauber@ucsd.edu

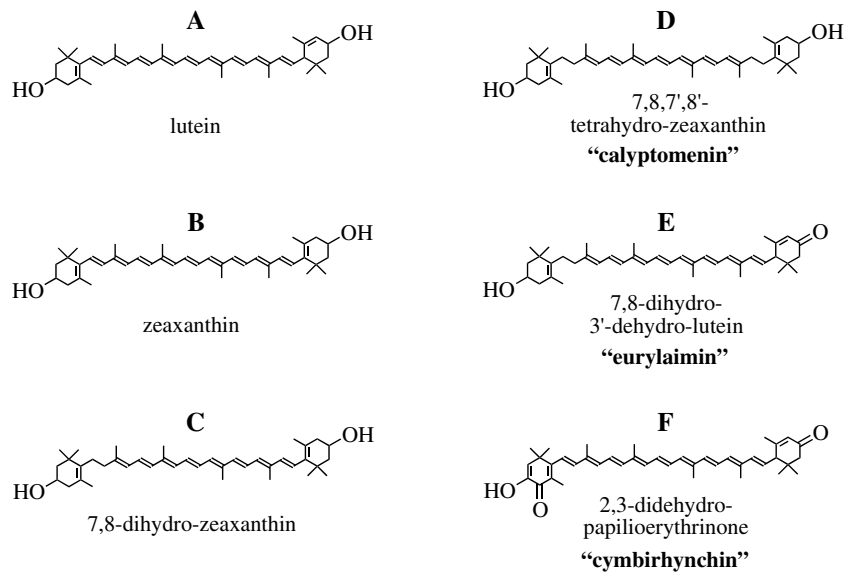
The yellow and green plumages of *Psarisomus dalhousiae* contain the unmodified dietary carotenoids lutein and zeaxanthin. The brilliant green feathers of *Calyptomena viridis* contain a mixture of lutein and two other xanthophylls that have previously been found only in woodpeckers (Picinae). The crimson and violet colors of *Cymbirhynchus*, *Sarcophanops*, and *Eurylaimus* are produced by a novel pigment, which is identified as 2,3-didehydro-papilioerythrinone. The molecular structure of this carotenoid was confirmed using <sup>1</sup>H nuclear magnetic resonance, correlated two-dimensional spectroscopy, and two-dimensional nuclear Overhauser effect spectroscopy. Resonance Raman (rR) spectroscopy carried out at room and low temperatures was used to probe the configuration and conformation of 2,3-didehydro-papilioerythrinone in situ within crimson *C. macrorhynchos* and purple-red *E. javanicus* feathers. The rR spectra reveal that the pigment is in an all-*trans* configuration and appears to be relatively planar in the feathers. The likely metabolic pathways for the production of broadbill carotenoids from dietary precursors are discussed.

**Keywords** Carotenoid metabolism · Feather coloration · High-performance liquid chromatography · Nuclear magnetic resonance · Pigment analysis · Resonance Raman spectroscopy

## Introduction

The non-structural red, orange, yellow, and pink plumage colors of most birds are produced by exogenous carotenoid pigments that are absorbed from the diet (McGraw 2006a). Many of these species of birds have evolved the capacity to metabolically alter simple dietary xanthophylls to produce new carotenoid molecules and create distinctive plumage

**Fig. 1** Molecular structures of carotenoids identified in broadbill plumage: **a** lutein, **b** zeaxanthin, **c** 7,8-dihydro-zeaxanthin, **d** 7,8,7',8'-tetrahydro-zeaxanthin (or calyptomenin), **e** 7,8-dihydro-3'-dehydro-lutein (or eurylaimin), and **f** 2,3-didehydro-papilioerythrinone (cymbirhynchin)



colorations. For example, 4-ketocarotenoids are produced metabolically by at least 22 families of birds (McGraw 2006a). A carbonyl group in the C4 (or C4') position effectively extends the conjugated chain into the end groups of the molecule, causing a redshift of the absorption relative to the typical dietary xanthophylls such as lutein and zeaxanthin, which lack keto groups (Fig. 1a, b). The colors associated with the ketocarotenoids in plumage are typically orange, red, or pink. Conversely, birds are also able to create unique lemon-yellow colors by saturating the double bond between C7 and C8, thus shortening the conjugated chain length and blueshifting the absorption of the molecule. These 7,8-dihydro-xanthophylls have been observed in the plumage of woodpeckers and were termed “picofulvins” (Stradi et al. 1998).

Recently, we discovered a new class of plumage ketocarotenoids in the largely frugivorous Neotropical bird family of cotingas (Cotingidae). These molecules are derived metabolically and share the unique structure of 3 (or 3,3')-methoxy groups on a 4-keto- $\beta$ -ring(s) (LaFountain et al. 2010). Additional structural variation among the seven new methoxy-ketocarotenoids depends upon whether the molecules are derived from  $\beta,\beta$ -ring or  $\beta,\epsilon$ -ring xanthophylls and whether the C2–C3 bond of each  $\beta$ -ring is saturated or unsaturated (LaFountain et al. 2010; Prum et al. 2012a). These methoxy-carotenoids were found in the plumage of twelve species within seven different cotinga genera (Prum et al. 2012a). A comparative phylogenetic analysis demonstrates that the expression of methoxy-carotenoids in plumage has evolved multiple times within Cotingidae, but it appears likely that the unique metabolic enzymes to produce these molecules may have had a single early evolutionary origin within the family. Reflectance spectroscopy and avian visual color space analysis reveal

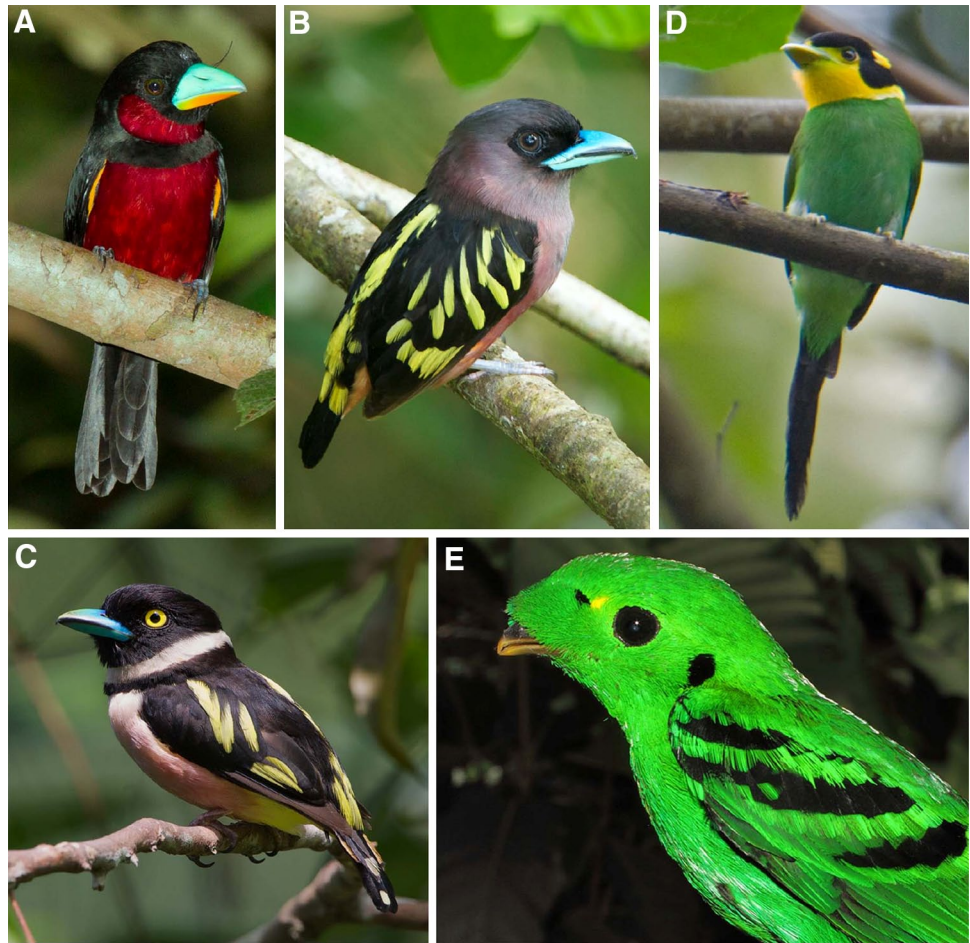
that methoxy-carotenoids produce distinctly saturated red and unique violet and purple plumage colors. Thus, cotingas provide a premier example of the evolution of diverse carotenoid metabolic capacity and molecular diversity for the achievement of unique plumage coloration.

The methoxy-ketocarotenoids and their interaction with the feather protein environment cause unique red, magenta, and purple hues in cotingas. We were eager to discover whether the plumage of birds in other families with similar coloration to the cotingas is also caused by methoxy-ketocarotenoids, or by other molecules with a different molecular structure.

The suboscine family of broadbills (Eurylaimidae) provides examples of plumage coloration that are both remarkably similar to the cotingas and quite distinct. The Black-and-red Broadbill (*Cymbirhynchus macrorhynchus*, Fig. 2a) of Southeast Asia has crimson throat and belly plumage, which is virtually identical in coloration to the methoxy-carotenoid throat patch of the Purple-throated Fruitcrow (*Querula purpurata*, Cotingidae). Furthermore, related to *Cymbirhynchus* are the genera *Eurylaimus* and *Sarcophanops*, which include three species with conspicuous pink, violet, or purple-maroon plumage patches that are also combined with light yellow regions (Fig. 2b, c). Other species within Eurylaimidae have plumage coloration that contrasts with that of the cotingas. The Green Broadbill (*Calyptomena viridis*, Fig. 2e) has unique, vivid green plumage that results from a combination of yellow pigmentation and structural color. The Long-tailed Broadbill (*Psarisomus dalhousiae*, Fig. 2d) displays yellow plumage on the throat, and green or blue plumage on the belly, back, and wings that is produced by a combination of pigmentary and structural color.

To characterize the pigments of Eurylaimidae plumage and the metabolic processes that are necessary for

**Fig. 2** Photographs of males of five of six broadbill species analyzed: **a** Black-and-red Broadbill *Cymbirhynchus macrorhynchos*, **b** Banded Broadbill *E. javanicus*, **c** Black-and-yellow Broadbill *Eurylaimus ochromalus*, **d** Long-tailed Broadbill *P. dalhousiae*, and **e** Green Broadbill *C. viridis*. Mindanao-Wattled Broadbill *Sarcophanops steerii* is not pictured. Photo Credits—**a** and **e** Kristof Zyskowski, **b–c** Bjorn Oleson, and **d** VIREO, Spike Baker



their synthesis from dietary precursors, bound plumage carotenoids were extracted and analyzed from nine plumage patches in six species within five genera of broadbills. Reflectance spectra of the plumage patches were also recorded. The pigments were identified by high-performance liquid chromatography (HPLC), mass spectrometry, MS/MS fragment analysis, chemical tests, visible absorption, and NMR spectroscopy; two molecules were found to be new. The configuration and conformation of the carotenoid within the crimson-red and purple-red feathers in *Cymbirhynchus* and *Eurylaimus* were probed in situ by resonance Raman (rR) vibrational spectroscopy. Plausible metabolic pathways for the production of these molecules have been inferred from common dietary carotenoids.

## Methods

### Feather specimens

Feathers were collected from six different species of broadbills (specimen identifications given in Table 1): red breast feathers from the Black-and-red Broadbill *Cymbirhynchus*

*macrorhynchos*; pink breast feathers and yellow flank feathers from the Black-and-yellow Broadbill *Eurylaimus ochromalus*; purple-maroon breast feathers and yellow back feathers from the Banded Broadbill *Eurylaimus javanicus*; violet breast feathers of the Mindanao-Wattled Broadbill *Sarcophanops steerii*; yellow throat feathers and green belly feathers from the Long-tailed Broadbill *P. dalhousiae*; and green belly feathers from the Green Broadbill *C. viridis* (Fig. 2). Specimens varied in known age from 45 to 95 years old, but some were of unknown age. All specimens were well preserved in the curated museum collection of the Yale Peabody Museum of Natural History. Those birds with the best preservation of the original visible hue (based on comparison with photos of living specimens) were selected for the present work.

### Pigment extraction

Feather carotenoids were extracted and analyzed using a protocol described previously (LaFountain et al. 2010). Briefly, feathers were washed by soaking in 100 mL of technical-grade ethanol for 15 min and then patted dry. This process was repeated using technical-grade hexanes.

**Table 1** Species, specimen identification and collection data, sample area and color, and sex of all specimens used

Species	Specimen	Collection date	Sample area	Color	Sex
<i>Cymbirhynchus macrorhynchos</i>	YPM 42776	29 Jun 1917	Breast	Crimson red	Male
	YPM 46787	19 May 1957	Breast	Crimson red	Female
	YPM 51831	3 May 1953	Breast	Crimson red	Male
	YPM 51833	3 Jul 1954	Breast	Crimson red	Female
	YPM 51840	5 Aug 1952	Breast	Crimson red	Male
	YPM 51841	3 Aug 1951	Breast	Crimson red	Female
	YPM 51846	19 Aug 1952	Breast	Crimson red	Male
	YPM 51847	Unknown	Breast	Crimson red	Female
	YPM 51848	2 Feb 1953	Breast	Crimson red	Male
	YPM 51856	23 Nov 1951	Breast	Crimson red	Male
	YPM 51859	19 May 1952	Breast	Crimson red	Male
	YPM 51863	23 July 1951	Breast	Crimson red	Female
	YPM 51865	2 Aug 1951	Breast	Crimson red	Female
	YPM 51900	11 Feb 1954	Breast	Crimson red	Male
<i>Eurylaimus ochromalus</i>	YPM 51915	10 April 1954	Breast, flank	Rosy pink, yellow	Female
	YPM 51932	4 Mar 1954	Breast, flank	Rosy pink, yellow	Male
	YPM 51938	5 Aug 1951	Breast, flank	Rosy pink, yellow	Male
<i>Sarcophanops steerii</i>	YPM 97073	6 June 1967	Breast	Purple-maroon	Male
<i>Eurylaimus javanicus</i>	YPM 46810	Unknown	Breast, back	Purple-maroon, yellow	Female
	YPM 63068	13 Dec 1954	Breast, back	Purple-maroon, yellow	Female
	YPM 63069	15 Jan 1953	Breast, back	Purple-maroon, yellow	Male
	YPM 63070	2 Feb 1953	Breast, back	Purple-maroon, yellow	Male
	YPM 63071	2 Feb 1953	Breast, back	Purple-maroon, yellow	Male
<i>Psarisomus dalhousiae</i>	YPM 17358	22 April 1939	Throat, belly	Yellow, green	Male
	YPM 17360	4 Sept 1940	Throat, belly	Yellow, green	Female
	YPM 17361	Unknown	Throat, belly	Yellow, green	unknown
	YPM 39776	3 Oct 1956	Throat, belly	Yellow, green	Female
<i>Calypotomena viridis</i>	YPM 51812	Unknown	Belly	Green	Male
	YPM 51819	25 Feb 1953	Belly	Green	Male
	YPM 51828	Unknown	Belly	Green	Unknown

After washing, the colored portions were removed with scissors, placed into 15-mL glass test tubes, and covered with acidified pyridine. The tubes were then placed into a 90 °C water bath until loss of pigmentation from the feathers appeared complete, which took anywhere from 30 min to 3 h. The acidified pyridine containing the carotenoid pigments was then added to a mixture of HPLC-grade methyl *tert*-butyl ether (MTBE) and water (3:1 v/v) for the purpose of removing both the acidified pyridine and relatively polar lipids (McGraw et al. 2005). The water layer was removed by pipette, and the organic solvent layer was washed with an equal amount of water two additional times. The MTBE phase was then dried under nitrogen gas, and the solid residue was re-dissolved in 14 % acetone in hexanes (v/v) for analysis using the previously described HPLC protocol (LaFountain et al. 2010).

#### High-performance liquid chromatography

High-performance liquid chromatography was conducted on a Waters 600E multi-solvent delivery system equipped with a Waters 2996 photodiode array detector. Initial HPLC analysis of feather extracts was carried out using a Phenomenex Luna normal phase (NP) silica column (5  $\mu$ m, 250  $\times$  4.6 mm). The mobile phase consisted of a linear gradient increasing from 10 % acetone in hexanes to 20 % acetone in hexanes over 40 min, with a flow rate of 1.5 mL/min. For preparative HPLC, a Waters Sunfire OBD silica prep column (5  $\mu$ m, 19  $\times$  100 mm) was used with the same gradient, but the flow rate was increased to 7 mL/min. The injection solvent in both cases was 14 % acetone in hexanes (v/v).

Prior to mass spectrometry described below, individual pigments were re-purified on the same HPLC system using

a reversed phase (RP) protocol. The RP chromatography separated components that co-eluted with a NP column and removed additional lipids. The RP protocol employed a Waters NovaPak C18 column (4  $\mu\text{m}$ , 300  $\times$  3.9 mm) and an isocratic delivery of 99 % solvent A, 1 % solvent B for 15 min followed by a linear gradient to 60 % solvent A, and 40 % solvent B over the next 25 min. Solvent A consisted of 87:10:3 (v/v/v) acetonitrile/methanol/water, while solvent B consisted of 100 % ethyl acetate. All HPLC solvents were purchased from Fisher Scientific (Pittsburgh, PA, USA).

#### Mass spectrometry and MS/MS analysis

Mass spectrometry was carried out on either a Fisons Quattro II mass spectrometer (MassLynx software), an Applied Biosystems QTRAP 4000 (AB analyst software), or an Applied Biosystems API 2000 (AB analyst software). All three instruments were outfitted with an atmospheric pressure chemical ionization (APCI) probe. Samples were introduced by direct injection into the Quattro II instrument with the following parameters: cone voltage, 15 V; probe temperature, 480 °C; and source temperature, 110 °C. Samples were injected using an infusion pump at a flow rate of 5–10  $\mu\text{L}$  into both the QTRAP 4000 and API 2000 with the following parameters: probe temperature, 350 °C; curtain gas, 10 psi; collision gas, low; nebulizer current, 2.0  $\mu\text{A}$ ; ion source gas, 30.0 psi; declustering potential, 60 V; and collision energy, 10 eV. Novel molecules from *C. macrorhynchos*, *Sarcophanops*, and *Eurylaimus* sp. were further subjected to analysis by MS/MS fragmentation. The instrument settings remained the same in MS/MS mode, with the exception that the collision energy was increased to 30 eV.

#### Nuclear magnetic resonance

Over one hundred red feathers were collected from multiple specimens of *C. macrorhynchos*, including seven male specimens (YPM 42776, 51831, 51840, 51846, 51848, 51856, and 51859) and five female specimens (YPM 51833, 51841, 51847, 51863, and 51865). The feathers were combined, and pigments were extracted and purified by HPLC as described above. The all-*trans* red pigment was collected, dried under nitrogen gas, and redissolved in chloroform-*d* (99.8 %, Cambridge Isotope Laboratories, Inc.). The sample was then analyzed on a Bruker AVANCE III 400 MHz NMR spectrometer using  $^1\text{H}$  spectroscopy, correlated two-dimensional spectroscopy (COSY), and two-dimensional nuclear Overhauser effect spectroscopy (NOESY). The NOESY spectra were the sum of 64 scans. The instrument parameters were as follows: spectral width, 4.084 kHz; power level 12 W; mixing time, 1.0 s; and delay, 2 s. The data were analyzed using the software program MestReNova v8.0.2 (Mestrelab Research).

#### Pigment identification and quantitation

Pigment identifications were based on a comparison of absorption spectra and HPLC retention times with bona fide standards as described in previous work (LaFountain et al. 2010). Mass spectrometry, chemical analyses by saponification, and sodium borohydride reduction (Eugster 1995) were used to provide additional support for the identifications as necessary.

Molar concentrations of the individual pigments were calculated by determining the integrated area of each HPLC peak at the detection wavelength of maximum absorbance and by taking into account the molar absorption coefficient. The molar concentration was then used to calculate the estimated mass (Schiedt and Liaaen-Jensen 1995). The calculated mass values of each individual pigment were then divided by that of the total mass of carotenoids to find the mass percentages. Molar absorption coefficients ( $\epsilon$ ) for novel carotenoids or for ones that do not have measured values were calculated using the reported values for carotenoids with the same number of conjugated carbon–carbon double bonds.

#### Saponification

Possible carotenoid esters within the red *C. macrorhynchos* and yellow *E. ochromalus* feather extracts were checked by hydrolysis with methanolic potassium hydroxide (KOH) following Eugster (Eugster 1995). Briefly, fresh feather extracts were divided into two separate glass vials, dried under nitrogen gas, and 1 mL of diethyl ether was then added to each vial to redissolve the sample. To one vial, 1 mL of 10 % methanolic KOH (w/v) was added for saponification. To the remaining vial, 1 mL of additional diethyl ether was added as a control. Esterified lutein was treated in the same manner to confirm the efficacy of the reagents. All samples were allowed to incubate in the dark at room temperature overnight. The following morning, 2 mL of water was added to the KOH-treated samples to stop the reaction. The ether layer was collected and dried. All samples were then subjected to HPLC analysis using the NP protocol described above.

#### Plumage reflectance measurement

The reflectance spectra of carotenoid patches from museum study skins were measured using an S2000 Ocean Optics spectrometer with an Ocean Optics DH-2000Bal deuterium–halogen light source (Ocean Optics, Dunedin, FL, USA). Reflectance was measured at normal incidence to the plumage using a bifurcated illumination/reflectance optical fiber. The optical fiber was held in an aluminum block that eliminated other illumination. The end of the fiber was held

approximately 6 mm above the plumage, and reflectance was measured from a circular patch of plumage 3 mm in diameter with an integration time of 500 ms. Reflectance spectra were recorded over the range 300–700 nm for each patch.

For each carotenoid plumage patch reflectance spectrum, we measured the wavelength at the reflectance slope midpoint,  $\lambda(R_{\text{mid}})$ :

$$\lambda(R_{\text{mid}}) = \lambda\left(\frac{R_{\text{max}} + R_{\text{min}}}{2}\right)$$

$\lambda(R_{\text{mid}})$  provides a measure of the wavelength position of the prominent transition in visible reflectance that characterizes these spectra of carotenoid plumage.

### Resonance Raman spectroscopy

Resonance Raman (rR) spectroscopy was employed to probe the carotenoid of the crimson *C. macrorhynchos* and purple-maroon *E. javanicus* feathers. The specific regions of the feathers that were probed were the barbules. The spectra were acquired at room temperature and at temperatures that approached the boiling point of liquid nitrogen (77 K).

Excitation beams at either 514.5 or 530.9 nm were generated by a mixed gas (argon/krypton) ion laser (Laser Innovations, Innova-70C). The beam was directed through a narrow-band interference filter (Semrock) that matched the wavelength of the laser line. The beam was then directed into a Zeiss Axio-Imager upright microscope that was modified in-house for rR spectroscopy. The excitation was focused onto the sample with a 0.55 NA objective lens. Scattered light was collected with the same lens and subsequently directed along a path that included a polarization scrambler and a sharp-cut edge filter (Semrock, RazorEdge) that was selected to block the excitation wavelength. The light was then focused onto the entrance slit of a 320-mm-focal length spectrograph equipped with 2,400 and 1,200 groove/mm holographic gratings and an open-electrode CCD detector (Horiba Jobin–Yvon, iHr-320 and Synapse). The slit width was 0.050 mm, which yielded a spectral resolution of  $\sim 3 \text{ cm}^{-1}$  with the 2,400 grooves/mm grating, and  $\sim 6 \text{ cm}^{-1}$  with the 1,200 grooves/mm grating.

Room temperature rR spectra were collected with 530.9 nm excitation and utilized the 1,200 grooves/mm grating. The power at the sample point was  $\sim 24 \mu\text{W}$ , and the focused beam was approximately 1  $\mu\text{m}$  in diameter. Therefore, the irradiance at the sample was approximately  $3,000 \text{ W/cm}^2$ . Low-temperature rR spectra were acquired with a cold stage that was cooled with liquid nitrogen (Linkam, THMS600). Barbs were cut from a feather and placed between two glass coverslips. Thin layers of silicon oil were used to hold the pair of coverslips and feather

in place and to improve thermal conduction to the cooling block. The temperature of the cold block was 78 K, as measured by an internal probe and indicated by the Linkam software. The THMS600 is designed to have the sample and cold block in the environment of dry nitrogen at ambient pressure; however, to better equilibrate the temperature of the sample with that of the cold block, a rough vacuum was pulled on the sample compartment. Thus, it is expected that the temperature of the sample is similar to that of the cold block. The low-temperature experiments utilized 514.5 nm excitation with  $\sim 150 \mu\text{W}$  power at the sample. A cylindrical lens (f.l. 150 mm) was inserted prior to the microscope so that the beam at the sample was defocused along one dimension. Therefore, despite the higher average power used to acquire the spectra at low temperature, the irradiance at the sample was estimated to be 10–20 times lower than for the room temperature spectroscopy. The grating used for the low-temperature spectra had 2,400 grooves/mm.

### Results

High-performance liquid chromatography analyses of the feather pigment extracts from the six species established that a single pigment was primarily responsible for the yellow patches in *E. ochromalus* and *E. javanicus* (Fig. 3; Table 2) and that a different single pigment was primarily responsible for the crimson, violet, and purple-maroon

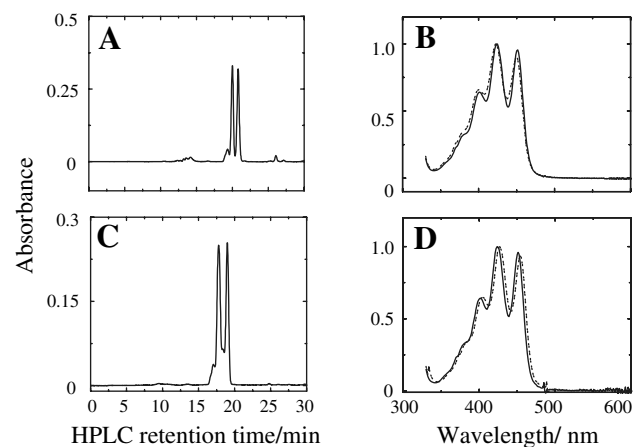


**Fig. 3** HPLC chromatograms of yellow feather extracts: **a** *E. ochromalus* feather extract HPLC chromatogram and **b** UV/Vis absorption spectra of the peaks at 20 min (solid line) and 21 min (dashed line); **c** *E. javanicus* feather extract HPLC chromatogram; and **d** absorption spectra of peaks collected at 17 min (solid line) and 19 min (dashed line). Both HPLC chromatograms are detected at 450 nm. All absorption spectra were measured by the photodiode array detector in the HPLC mobile-phase solvent (10–20 % acetone in hexanes) and have been normalized to 1

**Table 2** Mass percentages of pigments

Pigments <sup>a</sup>	<i>Cymbirhynchus macrorrhynchos</i> (red)	<i>Eurylaimus ochromalus</i> (yellow)	<i>Eurylaimus ochromalus</i> (pink)	<i>Sarcophanops steerii</i> (violet)	<i>Eurylaimus javanicus</i> (purple-maroon)	<i>Eurylaimus javanicus</i> (yellow)	<i>Psarisomus dalhousiae</i> (yellow)	<i>Psarisomus dalhousiae</i> (green)	<i>Calyptomena viridis</i> (green)
1	5						93	88	46
2							5	9	
3									6
4									47
5		88	5	100	100				
6	91	5	85	100		90			
7	4	7	10			10	2	4	1

<sup>a</sup> Pigments are designated as follows: (1) lutein, (2) zeaxanthin, (3) 7,8-dihydro-zeaxanthin, (4) 7,8,7',8'-tetrahydrozeaxanthin (or calyptomenin), (5) 7,8-dihydro-3'-dehydro-lutein (or eurylaimin), (6) 2,3-didehydro-papilioerythrinone (or cymbirhynchin), and (7) unidentified

patches in *C. macrorrhynchos*, *E. ochromalus*, *E. javanicus*, and *S. steerii* (Fig. 4). These two pigments are described in order, followed by the results from the analysis of the yellow pigments of *C. viridis* and *P. dalhousiae*.

**Yellow pigment from *Eurylaimus***

High-performance liquid chromatography of the pigment extracts collected from yellow *E. ochromalus* and *E. javanicus* feathers (Fig. 2b, c) both revealed two major peaks (Fig. 3a, c) which elute closely together and at a retention time similar to that of an astaxanthin standard. Therefore, we conclude that like astaxanthin, these pigments are relatively polar. The absorption spectra of the peaks observed at 20 and 21 min in the HPLC of *E. ochromalus* (Fig. 3a) and 17 and 19 min of *E. javanicus* (Fig. 3c) are nearly identical and have a high degree of vibronic structure with a  $\lambda_{max}$  of 423 nm (Fig. 3b, d). The resolved peaks in the absorption spectra in Fig. 3 correspond to transitions from the lowest vibronic level of the ground state (0) to different vibronic energy levels (0, 1, 2, etc.) of the excited state. The peaks are denoted (0–0) for the longest wavelength band, (0–1) which is usually the most intense band, and (0–2), (0–3), etc. Spectra of astaxanthin and other ketocarotenoids are different from these and typically have less-vibronically-resolved, or even featureless absorption spectra. The result suggests that there are no conjugated carbonyls in the carotenoids isolated here. The absorbance spectra are blueshifted relative to the common dietary carotenoids lutein and zeaxanthin, indicating that the yellow pigment within *E. javanicus* and *E. ochromalus* has fewer than the 10 or 11 conjugated double bonds found in dietary lutein and zeaxanthin, respectively. Based on a comparison with spectra reported for many other carotenoids (Britton 1995) in solvents with similar polarizability, the absorption spectra in Fig. 3 are most similar to those of carotenoids with 8 conjugated C=C bonds in the linear chain, or possibly with one additional conjugated bond in a  $\beta$ -ring (8 + 1). The best match is found for the former group, which has a 0–1 peak maximum in the range 421–423 nm. The number of carotenoids with 8 double bonds in the linear chain are relatively few in number and include  $\alpha$ -zeacarotene, flavoxanthin, latochrome, luteochrome, and 11',12'-dehydrononaprenoxanthin (Britton 1995) as well as the more recently identified 7,8-dihydro-xanthophyll, 7,8-dihydro-lutein (Stradi et al. 1998).

The two molecules isolated at 17 and 19 min from the *E. javanicus* feather extract (Fig. 3c) were analyzed by mass spectrometry which revealed the same mass of 568 *m/z* in APCI negative and positive modes (Fig. 5a). Thus, the two molecules are likely geometric isomers and are hereafter referred to as a single pigment. The absence of a *cis* band in either absorption spectra, which would appear ~140 nm

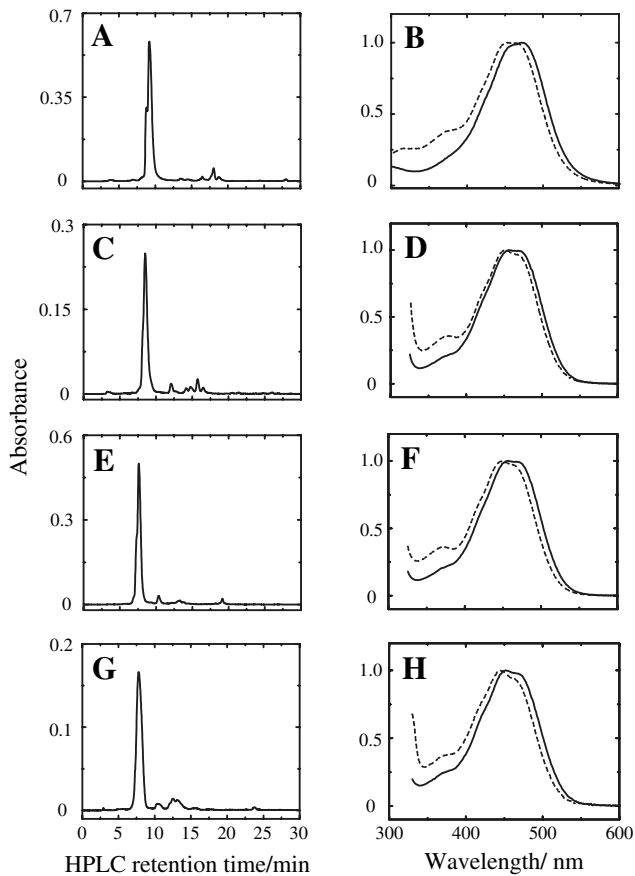


**Fig. 4** HPLC chromatograms of red, purple-maroon, and violet feather extracts: **a** *C. macrorhynchos* HPLC chromatogram and **b** absorption spectra of the *cis* isomer isolated at 8.8 min (dashed line) and all-*trans* pigment isolated at 9.2 min (solid line); **c** *E. ochromalus* HPLC chromatogram and **d** absorption spectra of the *cis* isomer isolated at 8.2 min (dashed line) and all-*trans* pigment isolated at 8.5 min (solid line); **e** *S. steerii* HPLC chromatogram and **f** absorption spectra of the *cis* isomer isolated at 7.3 min (dashed line) and all-*trans* pigment isolated at 7.6 min (solid line); and **g** *E. javanicus* HPLC chromatogram and **h** absorption spectra of the *cis* isomer isolated at 7.3 min (dashed line) and all-*trans* pigment isolated at 7.5 min (solid line). All HPLC chromatograms are detected at 450 nm. Absorption spectra were measured by the photodiode array detector in the HPLC mobile-phase solvent and have been normalized to 1

blueshifted from the  $\lambda_{\max}$  (Vetter et al. 1971) and the similarity of the spectra suggest that isomerization occurs at the terminal C9–C10 double bond of the chromophore.

This yellow pigment was collected and combined from multiple specimens of both *E. javanicus* and *E. ochromalus* in order to obtain a sufficient amount of material for MS/MS analysis. MS/MS analysis revealed some characteristic carotenoid fragments (Fig. 5b), including 567 [M-1] (loss of a hydrogen), 549 [M-1-18] (loss of hydroxyl), 475 [M-92] (toluene), 461 [M-107] (xylene), 203, and 137 (van Breemen et al. 2012). The 203 *m/z* fragment is indicative of at least one  $\beta$ -ring (Enzell and Back 1995) as described

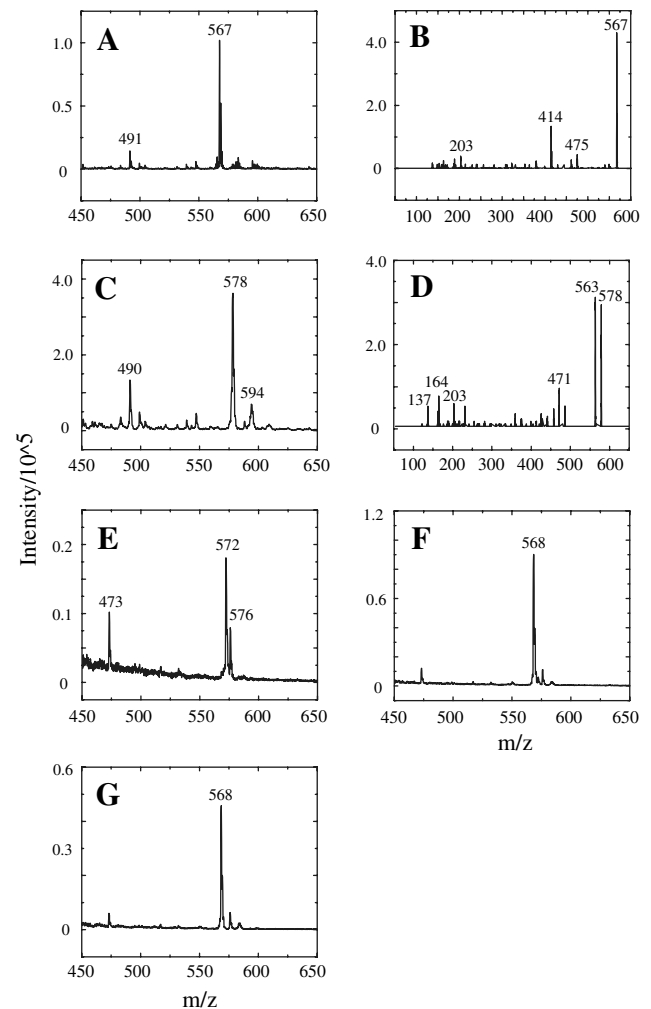


**Fig. 5** Mass spectra of **a** yellow pigment isolated from *E. javanicus* extract and **b** corresponding MS/MS fragmentation of 567 *m/z* ion; **c** red pigment isolated from *C. macrorhynchos* and **d** corresponding MS/MS fragmentation of 578 *m/z* ion; pigments isolated from *C. viridis* at **e** 21 min and **f** 24 min; and **g** pigment isolated from yellow *P. dalhousiae* feathers at 25 min. All of the spectra shown were measured in APCI negative mode

further below. The 137 *m/z* fragment could indicate either a  $\beta$ - or  $\epsilon$ -ring and is a fragment seen for zeaxanthin or lutein. Losses of 92 and 106 mass units are associated with the formation of toluene and xylene, respectively, from the polyene chain (Enzell and Back 1995; van Breemen et al. 2012). Another notable fragment is 414 [M-1-153]. M-153 has been associated with a 3-hydroxy, 7,8-dihydro- $\beta$ -ring (Enzell and Back 1995). This ion fragment was also reported by Stradi et al. (1998) in their report on the identification of 7,8-dihydro-xanthophylls in woodpeckers.

Treatment of the yellow pigment with sodium borohydride ( $\text{NaBH}_4$ ) did not significantly shift the absorption spectrum. However, the  $\text{NaBH}_4$ -treated sample yielded two separate chromatographic peaks of similar intensity



that eluted 5 and 7 min following the astaxanthin control, indicating that two different molecules, presumably isomers, were formed upon reduction. The identities of these two reduction products are unknown, and attempts to perform mass spectrometry on them were inconclusive due to low concentration. However, based on the observations that borohydride treatment (1) caused no substantial shift in the absorption spectra and (2) the reduced molecules eluted at longer retention times (i.e., were more polar than the untreated molecule), we can conclude that the yellow pigment has at least one carbonyl which is not conjugated with the polyene.

Saponification resulted in complete degradation of the pigment. Therefore, nothing can be concluded regarding the presence or absence of ester groups. It should be noted that 3-hydroxy- $\beta,\epsilon$ -carotene-3'-one, which has a lutein-like structure with a carbonyl group in the 3'-position of the  $\epsilon$ -ring, has also been reported to be unstable in the presence of bases (Buchecker and Eugster 1979; Britton et al. 2004). By contrast, lutein is stable in basic conditions, and derivatives with ester groups at the C3 and C3' position are reliably saponified by this method. Therefore, this suggests that an  $\epsilon$ -ring with a carbonyl at position C3 may be responsible for the instability under alkaline conditions.

Based on the evidence above, the yellow pigment from *E. javanicus* and *E. ochromalus* has a conjugation length of 8 and appears to be structurally similar to the 7,8-dihydro-xanthophylls, 7,8-dihydro-lutein, 7,8-dihydro- $\beta$ -cryptoxanthin, and 7,8,7',8'-dihydrozeaxanthin (Stradi et al. 1998). The mass spectral fragmentation pattern provides support for a single bond between C7 and C8. However, the mass of 7,8-dihydro-lutein is 570  $m/z$ , rather than the 568  $m/z$  mass of the yellow pigment. The 2-unit mass difference can be accounted for by the substitution of a hydroxyl group for a carbonyl group. While it is mathematically possible to account for the mass of the yellow pigment by oxidation of either one of the hydroxyl groups on the  $\epsilon$ - or  $\beta$ -rings to form keto groups, the presence of the M-153 fragment in the mass spectrum strongly suggests that the affected hydroxyl group is the one on the  $\epsilon$ -ring. We therefore propose that the yellow pigment is the novel carotenoid, 7,8-dihydro-3'-dehydro-lutein (Fig. 1e), and its full name is 7,8-dihydro-3-hydroxy- $\beta,\epsilon$ -carotene-3'-one. We propose that this newly identified carotenoid be referred to as eurylaimin, after the genus name of the birds with plumage containing this pigment, *Eurylaimus*.

To provide additional support for the identification of the yellow pigment from *E. javanicus* and *E. ochromalus* as 7,8-dihydro-3'-dehydro-lutein, we collected canary xanthophyll A (3'-hydroxy- $\epsilon,\epsilon$ -caroten-3-one) from the yellow plumage of an unrelated bird species (*Ptilinopus solomonensis speciosus*), purified it by HPLC, and analyzed it by mass spectrometry. The structure of canary xanthophyll

A is similar to that of 7,8-dihydro-3'-dehydro-lutein, in which both carotenoids have a carbonyl group in the C3 (or C3') position which is not conjugated with the polyene chain. The canary xanthophyll A sample was subjected to reduction by borohydride and MS/MS analysis, in order to observe the results of a known carotenoid with an unconjugated carbonyl. Like the yellow pigment from *E. javanicus* and *E. ochromalus*, reduction in canary xanthophyll A showed only a minimal shift (~2 nm) of its absorption spectrum and displayed two separate peaks of similar intensity in the HPLC. MS/MS fragmentation of the molecule resulted in several of the same ions observed from the yellow pigment, including M-18, M-92, M-189, 203, 188, and 137, indicating that these two molecules have many structural similarities. Notably missing from the canary xanthophyll A pigment was the M-153 fragment, providing further support that this species is an indicator of the 3-hydroxy, 7,8-dihydro-beta-ring in eurylaimin.

Crimson-violet pigment from *Cymbirhynchus*, *Eurylaimus*, and *Sarcophanops*

The HPLC analysis of the crimson, violet, and purple-maroon feathers from *C. macrorhynchus*, *E. ochromalus*, *E. javanicus*, and *S. steerii* (Fig. 2a–c) revealed a single pigment (Fig. 4a, c, e, g), which co-elutes with a *cis* isomer. These peaks have a retention time of ~8 min, which is slightly longer than that of a canthaxanthin standard but less than that of the yellow *Eurylaimus* pigment, indicating that this pigment is less polar than the latter. The absorption spectrum of the red pigment (Fig. 4b, d, f, h) lacks the vibronic structure of the yellow pigment (Fig. 3b, d) and resembles that of a carotenoid having one carbonyl in the  $\pi$ -electron conjugated chain. The isomer is identified as such based on the slight spectral blueshift and the “*cis*” peak in the absorption spectra at ~360 nm (Fig. 4b, d, f, h). The vibronic bands in the absorption spectrum for the all-*trans* isomer are not well resolved, but small features can be discerned at ~450 nm which corresponds to the (0–1) vibronic transition, and ~470 nm which corresponds to the longest wavelength (0–0) vibronic band. The spectrum is clearly blueshifted relative to carotenoids having two  $\beta$ -rings and two carbonyls at the C4, C4' positions fully conjugated with the linear chain (e.g., astaxanthin or adonirubin, each with 13 conjugated double bonds;  $\lambda_{\max}$  of astaxanthin is ~470 nm). It is also slightly blueshifted relative to carotenoids with two  $\beta$ -rings and only a single carbonyl at C4 (e.g., echinenone, 12 conjugated double bonds;  $\lambda_{\max}$  ~460 nm). The position matches most closely with those that have conjugation extending only to a single ring, i.e., where one  $\epsilon$ -ring is present. The candidates include those where the  $\beta$  conjugation extends only to a carbonyl in the 4-position (as in fritschiellaxanthin) or to the carbonyl and

a C2–C3 double bond (as in  $\alpha$ -doradecin, 12 conjugated double bonds) (Britton 1995).

The mass of the red pigment was found to be 578  $m/z$  (Fig. 5c). MS/MS of the 578  $m/z$  ion in negative mode (Fig. 5d) resulted in several fragment ions, including 563 [M-15], 486 [M-92] (toluene), 471 [M-1-106] (xylene), 375 [M-203], 203, 187, 164, and 137. The loss of 15 mass units has been reported to be associated with the loss of a methyl radical from zeaxanthin (van Breemen et al. 2012). The 203 and 375  $m/z$  fragments are indicative of at least one  $\beta$ -ring (Enzell and Back 1995) and are very commonly seen as fragments originating from  $\beta$ -carotene (Enzell and Back 1995; van Breemen et al. 2012),  $\alpha$ -carotene (van Breemen et al. 2012), astaxanthin (van Breemen et al. 2012),  $\beta$ -cryptoxanthin (van Breemen et al. 2012), and canthaxanthin (Enzell and Back 1995; LaFountain et al. 2010). The 137 and 187  $m/z$  fragment ions have been associated with zeaxanthin where the former originates from a  $\beta$ -ring and the latter comes from the polyene chain (van Breemen et al. 2012). The fragment ion 163  $m/z$  remains unidentified at this time.

Reduction by sodium borohydride causes a blueshift of  $\sim 17$  nm and a sharpening of the vibronic structure which is consistent with the presence of one conjugated carbonyl in the molecule. The chromophore of the reduction product is similar to that of  $\alpha$ -carotene. Therefore, we can deduce that this pigment has one carbonyl in the  $\pi$ -electron conjugation and potentially more that are out of conjugation with the polyene chain. Like the yellow pigment, the red pigment was not stable in methanolic KOH. Therefore, nothing can be concluded regarding the presence or absence of ester linkages.

The molecule 2,3-didehydro-papilioerythrinone (Fig. 1f) is consistent with the data presented above. The 12 conjugated double bonds of this structure are fully consistent with the candidates that were mentioned above in the context of absorption spectroscopy. A 1,2-diketo form is also a conceivable structural isomer; however, the tautomer is considered highly unlikely for this molecule, as it is for astacene (discussed below). We propose the name cymbirhynchin for 2,3-didehydro-papilioerythrinone (Fig. 1f), after the broadbill genus *Cymbirhynchus*, one of the three genera in which it has been found.

To confirm the identification of cymbirhynchin, we performed  $^1\text{H}$  and two-dimensional NMR spectroscopy. The  $^1\text{H}$ -NMR spectrum of the red pigment isolated from the combined feathers of twelve *C. macrorhynchus* specimens (Fig. 6) showed peaks in the range 6.0–6.8 ppm, the majority of which represent olefinic protons. The olefinic region of the spectrum included a singlet at 6.07 ppm, which is identified as the lone proton on C2 (Englert 1995) (Fig. 6b). Another singlet observed at 6.42 is consistent with the reported value for the proton on a hydroxyl group

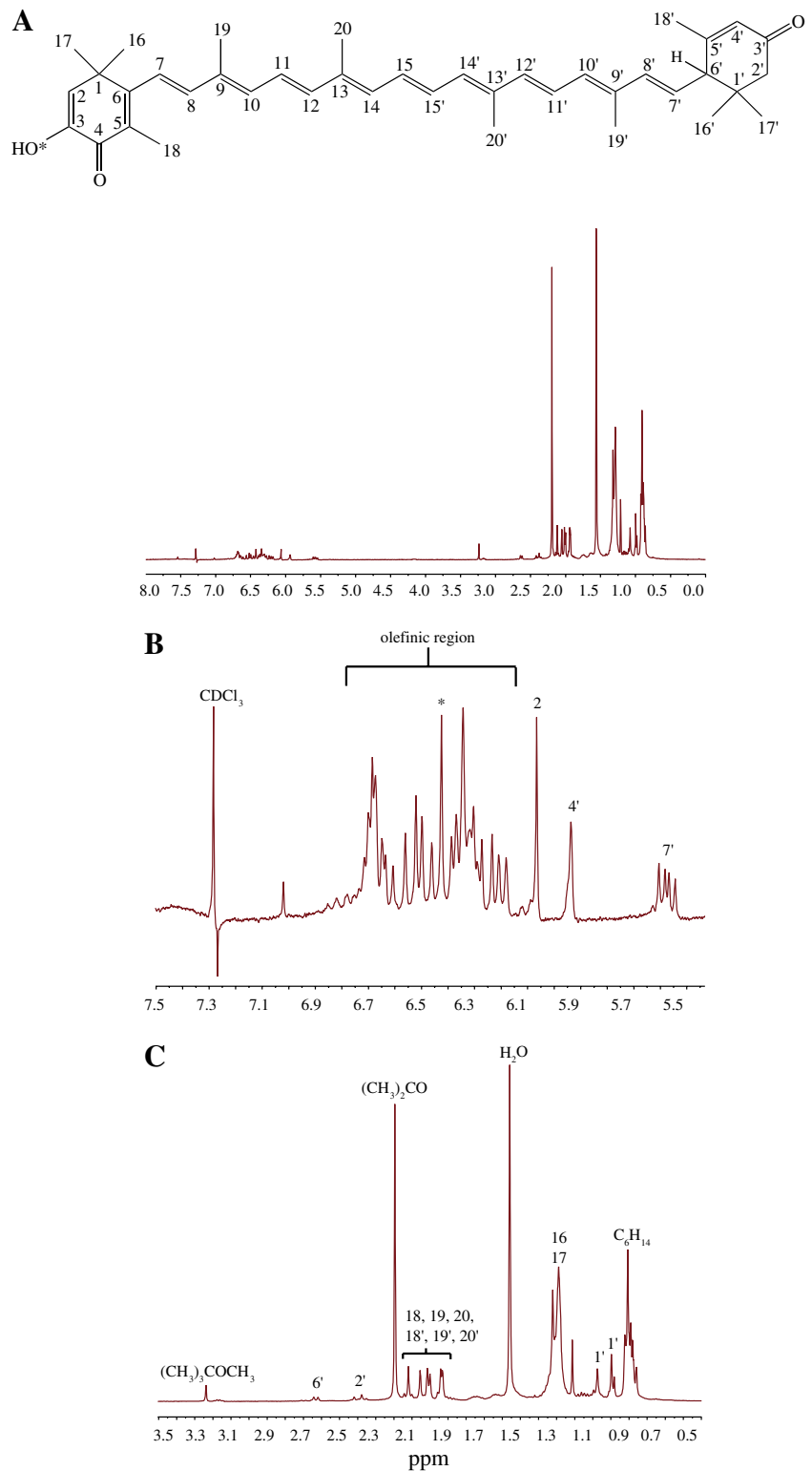
attached to C3 of a  $\beta$ -ring, with C3 having no other protons attached (Englert 1995). This indicates the presence of a 2,3-didehydro-3-hydroxyl-4-keto- $\beta$ -ring in the structure (Fig. 6). The  $^1\text{H}$ -NMR spectrum also revealed doublets at 2.1 and 2.4 ppm, each with a spin coupling frequency of 16.3 Hz. The 2D-COSY analysis confirmed that these two doublets are coupled and, based on comparison with published values (Englert 1995), belong to axial and equatorial ( $\alpha$  and  $\beta$ ) protons on C2' of the  $\varepsilon$ -ring. Another doublet was observed at 2.63 ppm with a spin coupling frequency of 9.4 Hz, which is identified as the proton on C6' of the  $\varepsilon$ -ring (Englert 1995). This doublet was found to be associated with a doublet of doublets at 5.57 ppm, which represents the proton on the neighboring carbon, C7'. The doublet of doublets at 5.57 ppm was further found to be associated with a doublet at 6.27 ppm, which represents the proton on C8' (Englert 1995). These couplings between the protons on C7' and C6', with frequencies of 9.5 and 15.5 Hz, respectively, are consistent with published reports for an  $\varepsilon$ -ring end group (Englert 1995). The two peaks at 1.07 and 0.9 ppm represent the six protons on the methyl groups attached to C1', C16', and 17' (Englert 1995). Integration of the peaks in the  $^1\text{H}$  spectrum (Fig. 6a) yielded results consistent with the values expected for the structure given in Fig. 6. Homonuclear 2D COSY analysis confirmed the predicted exchanges of neighboring protons in the vicinity of the  $\varepsilon$ -ring, including exchanges of the protons between C6' and C7', C7' and C8', and C4' and C18' and of the two protons on C2'. (See Fig. S1 in Supplemental Information, and the structure in Fig. 6).

Analysis using 2D NOESY also confirmed several proton interactions in the proposed structure (Fig. 7). With regard to the  $\beta$ -ring end group, NOESY revealed several spatial proton exchanges, including exchanges between the hydroxyl group on C3 with water; the lone proton on C2 with the protons of the methyl groups on C1 (C16 and C17), the proton on C7 with those of the methyl groups on C1 (C16 or C17), and the protons of the methyl group on C5 (C18) with the proton on C8. With regard to the  $\varepsilon$ -ring end group, NOESY revealed the spatial interactions between the axial and equatorial protons on C2', the proton on C4' with the protons on the methyl group of C5' (C18'), the protons on C18' with the proton on C6', and the lone proton on C6' with those of the methyl groups on C1' (C16' or 17').

#### Resonance Raman spectroscopy of the crimson-purple pigment

The variation in the colors of the cymbirichin plumages of *Cymbirhynchus*, *Eurylaimus*, and *Sarcophanops* species implies that additional features of the protein environment of the feathers alter the pigment absorption in situ. We examined this hypothesis with rR spectroscopy of the

**Fig. 6** Proposed structure of the red pigment, 2,3-didehydropapilioerythrinone, with carbons denoted numerically according to the scheme outlined in (Britton et al. 2004). **a** Complete  $^1\text{H-NMR}$  spectrum of the red pigment isolated from *C. macrorhynchos*, **b** close-up of the region from 5.5 to 7.5 ppm, **c** and close-up of the region between 0.5 and 3.5 ppm. The numbered peaks indicate the location of the proton on specific carbon atoms. The asterisk (\*) in **b** represents the proton of the hydroxyl group attached to C3. The spectrum also showed peaks belonging to the solvents used in sample preparation, including hexane (0.9 ppm), water (1.5 ppm), acetone (2.2 ppm), and methyl *tert*-butyl ether (MTBE) (3.2 ppm) (Gottlieb et al. 1997)

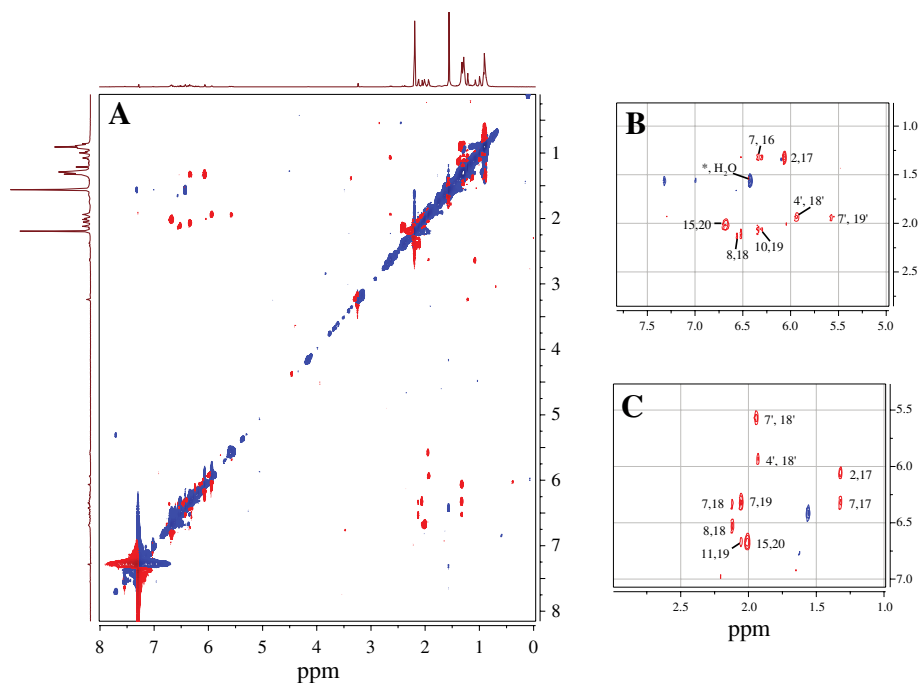


crimson red feathers of *C. macrorhynchos* and the purple-maroon feathers of *E. javanicus*.

The spectra of feathers acquired at room temperature and with high irradiance ( $\sim 3,000 \text{ W/cm}^2$ ) are very similar to those acquired at temperatures near 77 K and with less than

$300 \text{ W/cm}^2$ . The correspondence provides some reassurance that photodegradation is unlikely in these experiments. The robustness of the feathers to relatively high-irradiance excitation agrees with similar findings reported in a pioneering rR study of bird feathers (Veronelli et al. 1995).

**Fig. 7 a** Complete 2D-NOESY spectrum of the red pigment isolated from *C. macrorhynchos* with NOE interactions shown in red. Autocorrelation peaks are shown in blue. Specific regions of the spectrum are highlighted in **b** and **c**. The numbered peaks indicate the location of the proton on specific carbon atoms which are identified in Fig. 6. The asterisk (\*) in **b** represents the proton of the hydroxyl group attached to C3 (color figure online)



The rR spectra of the crimson red *C. macrorhynchos* and the purple-maroon *E. javanicus* feathers (Fig. 8) show the familiar signatures of carotenoids (Saito et al. 1983; Koyama and Hashimoto 1993; Koyama 1995; Veronelli et al. 1995; Robert 1999). The strongest band is an ethylenic ( $\nu_1$ ) band, and the peak frequency of *E. javanicus* ( $1,516\text{ cm}^{-1}$ ) is  $3\text{ cm}^{-1}$  lower than that of *C. macrorhynchos* ( $1,519\text{ cm}^{-1}$ ). The difference in the peak frequency is the same at low temperature, because the bands of both feathers upshift by  $2\text{ cm}^{-1}$  upon cooling. The fingerprint region ( $1,100\text{--}1,400\text{ cm}^{-1}$ ) consists of bands that are largely C–C single-bond stretches, in combination with C–H in-plane bends. One can generally identify bands that correspond closely for the two feathers, either within the pair of room temperature spectra or within the low-temperature pair. The most prominent band ( $\nu_2$ ) in the fingerprint region has a maximum at  $1,160\text{ cm}^{-1}$  that is identical for both feathers. This frequency is maintained at low temperatures. The strong intensity of this band as well as the lack of significant intensity in bands that are signatures of various *cis* isomers of  $\beta$ -carotene or other carotenoids (e.g.,  $1,140$ ,  $1,245$ , and  $1,274\text{ cm}^{-1}$ ) (Koyama et al. 1988; Koyama 1995; Koyama and Fujii 1999) indicates that the chromophore in both feathers is in the all-*trans* configuration. In the spectral region below  $1,100\text{ cm}^{-1}$ , the strongest band is  $\nu_3$  which is assigned to methyl rocking motions. The  $\nu_3$  band of both feathers is centered at the same frequency ( $1,011\text{ cm}^{-1}$ ) at room temperature (Fig. 8) or nearly the same frequency ( $1,007$  and  $1,008\text{ cm}^{-1}$ ) at low temperature. The bands at  $872$  and  $967\text{ cm}^{-1}$  are signatures of the hydrogen out-of-plane (HOOP) wagging

modes. The matching intensities of these bands suggest that the degree of planarity is similar for the carotenoids of both feathers (Eyring et al. 1982; Saito et al. 1983; Curry et al. 1984; Robert 2009).

There are a couple of weak bands that are possibly specific indicators of the C–O and C=O modes of 2,3-didehydro-papilioerythrinone. Bands that represent significant C–O stretching character are expected to have a frequency in the range  $1,000\text{--}1,100\text{ cm}^{-1}$ . For example, astaxanthin has a strong IR absorption band at  $1,074\text{ cm}^{-1}$  which has been assigned to a C–O stretch (Bernhard and Grosjean 1995). Similarly, astacene has a strong absorption band at  $1,062$  or  $1,063\text{ cm}^{-1}$  that is assigned to a C–O stretch (Bernhard and Grosjean 1995). In our rR spectra of feathers, a very weak band is found with maximum in the range  $1,062\text{--}1,065\text{ cm}^{-1}$ . Although this feature is small in each spectrum, it is possibly the signature of a C–O stretch that is expected for the –enol form of the carotenoid. No other modes of an all-*trans* carotenoid are expected to occur in this region, though *cis* isomers could have overlapping bands (Koyama et al. 1988). Next, bands at  $1,602/1,605\text{ cm}^{-1}$  (*E. javanicus*) and  $\sim 1,624\text{ cm}^{-1}$  (*C. macrorhynchos*) are possibly signatures of the C=O stretch of the conjugated ketone. These frequencies are unusually low for a carbonyl stretch; however, an intramolecular hydrogen bond between the C=O and the nearby –OH group of the enol is expected to cause significantly lowering in frequency. Similarly, the C=O stretch of astacene ( $1,619\text{ cm}^{-1}$ ) is significantly lower than that of canthaxanthin ( $1,657\text{ cm}^{-1}$ ) or astaxanthin ( $1,653\text{ cm}^{-1}$ ) (Bernhard and Grosjean 1995).

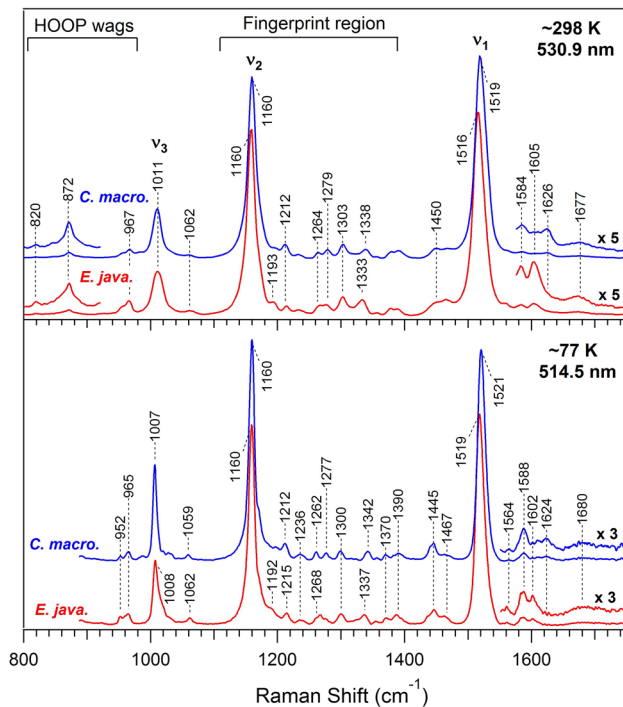


**Fig. 8** Resonance Raman spectra of isolated 2,3-didehydro-papilioerythrone in situ in the feathers of *C. macrorhynchos* (blue) and *E. javanicus* (red). The top frame shows the samples measured at room temperature with the excitation wavelength at 530.9 nm. The spectrum of each feather was acquired with 20 min of integration. The regions between 800 and 900  $\text{cm}^{-1}$  and 1,550–2,100  $\text{cm}^{-1}$  are magnified 5 $\times$ . The lower frame shows the spectra measured as the sample temperature approached 77 K (see text) and the excitation wavelength was 514.5 nm. The region between 1,550 and 1,800  $\text{cm}^{-1}$  is magnified 3 $\times$ .  $\nu_1$ ,  $\nu_2$ ,  $\nu_3$ , and the fingerprint region are labeled. Each spectrum was acquired with 15 min of integration, and the spectra are normalized for equal amplitudes of the ethylenic band (color figure online)

These collective results support the proposed enol structure of 2,3-didehydro-papilioerythrone (Fig. 6) and that the configuration in the feathers is all-*trans*.

#### Yellow *Calyptomena* pigment

The vibrant green plumage of *C. viridis* (Fig. 2e) is produced by a combination of spongy medullary barb structural color (Saranathan et al. 2012) and a yellow pigment that has not been previously identified. HPLC analysis of *C. viridis* feather extract reveals two major pigments, which elute at 21 and 24 min (Fig. 9a). The absorption spectrum of the first pigment has a very well-resolved vibronic structure. The relative absorbance of the third versus the second vibronic peaks—the %III/II value—provides a measure of the degree of spectral fine structure (Britton 1995). The %III/II value of 94 (Fig. 9b, solid line) for this pigment clearly indicates that there are no conjugated carbonyls. With a  $\lambda_{\text{max}}$

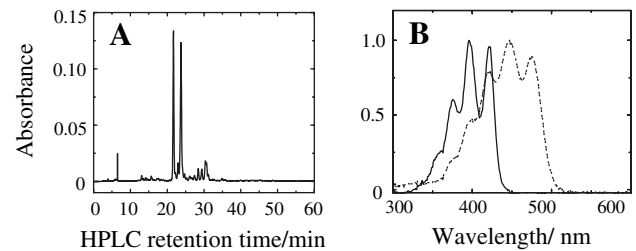


**Fig. 9** *C. viridis* a HPLC and b absorption spectra of pigments observed at 21 min (solid line) and 24 min (dashed line) measured in acetonitrile. HPLC is detected at 420 nm

of 397 nm, its conjugated chain length is shorter than all four carotenoids common in avian diets ( $\beta$ -carotene,  $\beta$ -cryptoxanthin, lutein, and zeaxanthin) and likely has seven conjugated carbon–carbon double bonds ( $n = 7$ ). The second major HPLC peak has the characteristic retention time and absorption spectrum of lutein (Fig. 9b, dashed line).

Between these two large peaks exists a small peak that has an absorption spectrum displaying a  $\lambda_{\text{max}}$  at 426 nm (spectrum not shown). A pigment with a similar absorption spectrum is also observed eluting along with the lutein peak and contributes to the shoulder in the vicinity of 400 nm. Based on known spectra of 7,8-dihydro- $\beta$ -carotene (Britton et al. 2004) and 7,8-dihydro- $\beta$ -cryptoxanthin (Stradi et al. 1998), this absorption spectrum is consistent with a carotenoid having  $n = 9$ . Therefore, this pigment likely represents an intermediate between a dietary carotenoid and one with the blueshifted spectrum in Fig. 9b, potentially a 7,8-dihydro-xanthophyll.

The two major pigments from the HPLC were analyzed in APCI negative mode and were found to have masses of 572 and 568  $m/z$ , respectively (Fig. 5e, f). Insufficient concentrations of either peak were available for subsequent analysis by MS/MS fragmentation.

Based on this cumulative data, the two major pigments are identified as a 7,8,7',8'-tetrahydro-xanthophyll (of either lutein or zeaxanthin) and unmodified lutein (Fig. 1a). It is difficult to distinguish 7,8,7',8'-tetrahydro-lutein from 7,8,7',8'-tetrahydro-zeaxanthin. However, based on our data, and a comparison with previous findings for the same chromophore by Stradi et al. (1998), it is very likely that this pigment is 7,8,7',8'-tetrahydro-zeaxanthin (Fig. 1d). We propose the name calyptomenin for this pigment, after the broadbill genus *Calyptomena*.

The mass percentages of these pigments were as follows: 7,8,7',8'-tetrahydro-zeaxanthin 47 %; 7,8-dihydro-zeaxanthin, 6.2 %; lutein (and isomers), 45.6 %; and unknown, 1 % (Table 2). It is important to note that these values are biased slightly in favor of lutein, due to the co-elution of 7,8-dihydro-zeaxanthin with the major lutein peak.

### Yellow *Psarisomus* pigment

High-performance liquid chromatography analysis of the extract from yellow *P. dalhousiae* throat feathers (Fig. 2d) revealed one major peak eluting at 25 min and having an absorption spectrum with a  $\lambda_{\text{max}}$  at 447 nm (Fig. 10a), both features of which are consistent with lutein. The small peak that elutes immediately after lutein at 26 min appears to be zeaxanthin, based on the retention time and absorption spectrum. Minor peaks were observed between 29 and 34 min (Fig. 10a), which also have absorption spectra consistent with lutein, and are therefore very likely cis isomers which could be formed during the extraction process.

The major peak collected at 25 min (Fig. 10a, b) yielded a mass of 568 *m/z* (Fig. 5g), thus confirming the identity of the primary pigment to be lutein. The mass percentages of lutein and the minor pigments are as follows: lutein and cis isomers, 93 %; zeaxanthin, 5 %; and unknown, 2 %.

High-performance liquid chromatography analysis of green belly feathers of *P. dalhousiae* (Fig. 2d) showed a similar elution profile (Fig. 10c) to that of the yellow feathers (Fig. 10a). The retention time and absorption spectrum (Fig. 10d) of the major pigment observed at 24 min match those of lutein in the yellow *P. dalhousiae* feathers. Therefore, this pigment is identified as lutein without further analysis. A small peak observed eluting immediately after lutein at 24.5 min is very likely that of zeaxanthin based on previous studies. The other minor peaks observed between 28 and 35 min are likely *cis* isomers formed during the extraction procedure. The mass percentages for the pigments of the green feathers were as follows: lutein and cis isomers, 88 %; zeaxanthin, 8 %; and unknown, 4 % (Table 2).

### Broadbill plumage reflectance spectra

The reflectance spectra of carotenoid plumages of broadbills are strongly correlated with their distinctive molecular structures (Fig. 11), particularly the length of the conjugated chain of carbon double bonds. The yellow pigment of *E. javanicus* and *E. ochromalus*, 7,8-dihydro-3'-dehydro-lutein or eurylaimin, is a 7,8-dihydro-xanthophyll with eight conjugated double bonds (Fig. 1). The reflectance spectra of eurylaimin plumages are predictably blueshifted in comparison with plumage containing typical xanthophylls with conjugation lengths of ten (e.g., lutein) or eleven (e.g., zeaxanthin). The reflectance spectra of the light chiffon-yellow plumages of *E. javanicus* and *E. ochromalus* have a slope midpoint value  $\lambda(R_{\text{mid}})$  of 475 nm (Fig. 11). In contrast, the yellow plumage of other bird species that are colored with only dietary xanthophylls has slope midpoint values that are 35 nm larger, for example, 509 nm (*Tijuca atra*, lutein), 511 nm (*Dendroica petechia*,

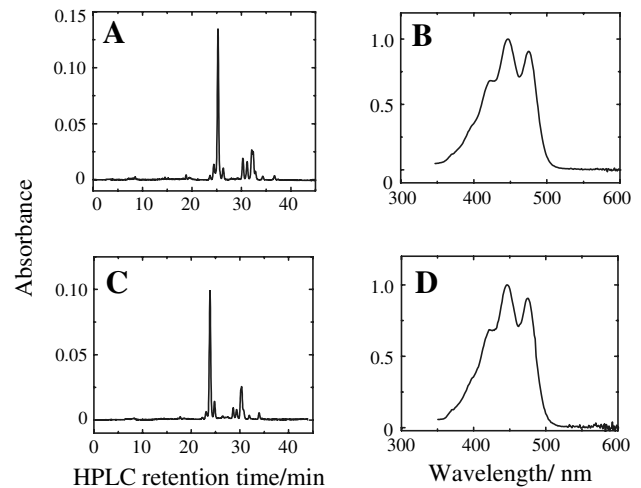


**Fig. 10** *Psarisomus dalhousiae* yellow feather extract **a** HPLC with **b** absorption spectrum of major peak at 25 min; and **c** HPLC of green *P. dalhousiae* extract with **d** absorption spectrum of peak isolated at 24 min. Both HPLC chromatograms are detected at 440 nm. Absorption spectra were collected by the photodiode array detector in the mobile-phase solvent and are normalized to 1

lutein), and 516 nm (*Oriolus xanthornus*, lutein and zeaxanthin) (McGraw 2006a; Prum et al. 2012a).

The reflectance spectra of the crimson patches of *C. macrorhynchos* and the purple-red plumage of *E. javanicus* have similar reflectance slope midpoints of 637 and 642 nm, respectively. This difference alone is unable to account for the observed variation in color. Another difference in the spectra is the amplitude of the reflectance in the blue-green region relative to the red region. The feathers from *C. macrorhynchos* have very low reflectance from 450 to 580 nm. In fact, the lowest reflectance (<5 %) is located in the visible region at ~500 nm. The reflectance is less than one-tenth the value at ~700 nm. Given that the blue, green, and yellow colors are apparently absorbed efficiently, it stands to reason that the color of the *C. macrorhynchos* breast appears deep red. In contrast, the reflectance of *E. javanicus* breast feathers is not only strong in the red region, but is also substantial in the blue-green region. The reflectance values (~20 %) in the range from 380 to 550 nm are approximately three or four times higher than the reflectance values of *C. macrorhynchos* in that region. The combination of blue and red reflection/scattering is consistent with a purple-red or maroon appearance of the breast feathers from *E. javanicus*. Other reflectance/scattering spectra (not shown) acquired from individual feathers can be analyzed to derive absorption spectra of the carotenoid in *C. macrorhynchos* and *E. javanicus*. The wavelength that is midway between the half-maxima on either side of the carotenoid absorption band is ~516 nm for *C. macrorhynchos*, versus 537 nm for *E. javanicus*.

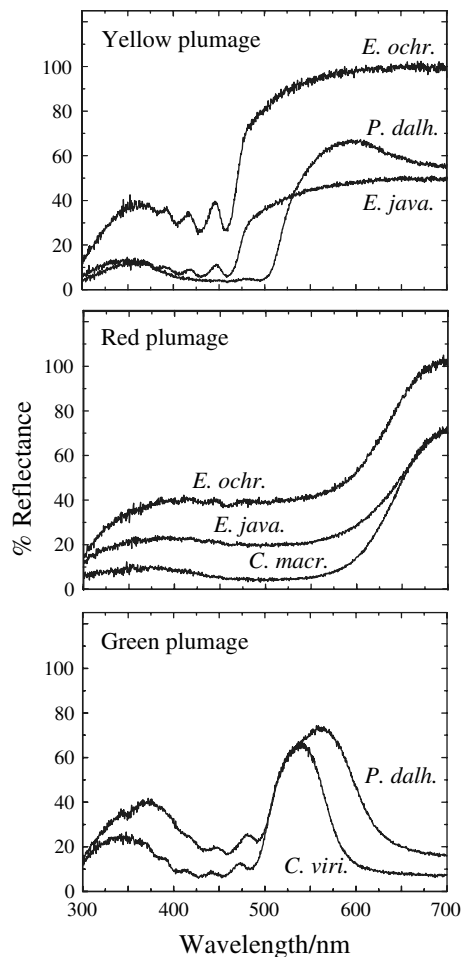


**Fig. 11** Reflectance spectra of broadbill yellow (top), red (middle), and green (bottom) plumage as detected by an S2000 Ocean Optics spectrometer with an Ocean Optics DH-2000Bal deuterium–halogen light source. *C. macr.*—*Cymbirhynchus macrorhynchus*; *C. viri.*—*Calyptomena viridis*; *E. java.*—*Eurylaimus javanicus*; *E. ochr.*—*Eurylaimus ochromalus*; and *Psda.*—*Psarisous dalhousiae*

Furthermore, by considering the intensity of the absorption of keratin at ~280 nm as an internal standard, it is clear that the concentration of carotenoid pigmentation is approximately twofold greater in the feathers from *C. macrorhynchus* relative to those from *E. javanicus*.

It should be noted that all feathers retained a pale orange hue after extraction of carotenoids, which is likely caused by melanin pigments (Hudon 1991a; McGraw et al. 2005, McGraw 2006b). The orange appearance specifically suggests pheomelanin. The absorption of this pigment monotonically declines across the 300–700 nm window (McGraw 2006b) that is of interest here. The extent to which pheomelanin contributes to the blue absorption/reflectance for *C. macrorhynchus* or *E. javanicus* was not explored.

The pigments of the yellow wing patch of *Sarcophanops steerii* were not analyzed here because this wing patch is

tiny and museum specimens of this species are rare. Interestingly, however, this plumage patch has an orange-yellow, rather than lemon-yellow, appearance and a reflectance slope midpoint value of 515 nm, which is typical of dietary xanthophylls. Thus, it is likely that the yellow wing patches of *Sarcophanops* are not produced by eurylaimin or another 7,8-dihydro-xanthophyll. Also, the green and yellow plumages of *C. viridis* and *P. dalhousiae* are both produced by a complex interaction of optical scattering and pigmentary absorbance that is beyond the scope of this study and will be dealt with in a future publication.

## Discussion

We have identified one ketocarotenoid, three 7,8-dihydro-xanthophylls, and unmodified dietary lutein and zeaxanthin from the plumages of six species of broadbills (Fig. 1). The yellow pigment from *E. javanicus* and *E. ochromalus* is identified as 7,8-dihydro-3'-dehydro-lutein, a new 7,8-dihydro-xanthophyll with a conjugated carbon double-bond chain length of  $n = 8$  (Fig. 1e). The red, violet, or purple-maroon pigment of *Cymbirhynchus*, *Eurylaimus*, and *Sarcophanops* is identified as 2,3-didehydro-papilioerythrinone, a new 4-ketocarotenoid molecule in which the  $\pi$ -electron conjugated chain length is 12 and extends to C2 within the  $\beta$ -ring (Fig. 1f). In *C. viridis*, the green plumage includes two 7,8-dihydro-xanthophylls identified as 7,8-dihydro-zeaxanthin and 7,8,7',8'-tetrahydro-zeaxanthin (Fig. 1c, d). The  $\pi$ -electron conjugation chain lengths of these molecules are 9 and 7, respectively. Lastly, the pigments within the yellow and green plumage patches of *P. dalhousiae* were predominately lutein with small quantities of zeaxanthin.

## Metabolic pathways for production of broadbill carotenoids

Of the six plumage carotenoids found in broadbills, two are common dietary xanthophylls and four are metabolically derived from dietary xanthophylls by the birds themselves. We hypothesize that these four plumage carotenoids can be produced from lutein and zeaxanthin in two or three metabolic steps using only four different enzymatic reactions (Fig. 12).

All these proposed enzymatic steps are previously known to occur in other groups of birds. For example, the production of eurylaimin (Fig. 12a) requires two metabolic processes— $\epsilon$ -hydroxyl-dehydrogenation and C7,8-dihydrogenation. The  $\epsilon$ -hydroxyl-dehydrogenation is also required in the production of canary xanthophylls from lutein (Stradi et al. 1995b, 1996, 1997; McGraw et al. 2001; McGraw 2006a), and the C7,8-dihydrogenation reaction is also used

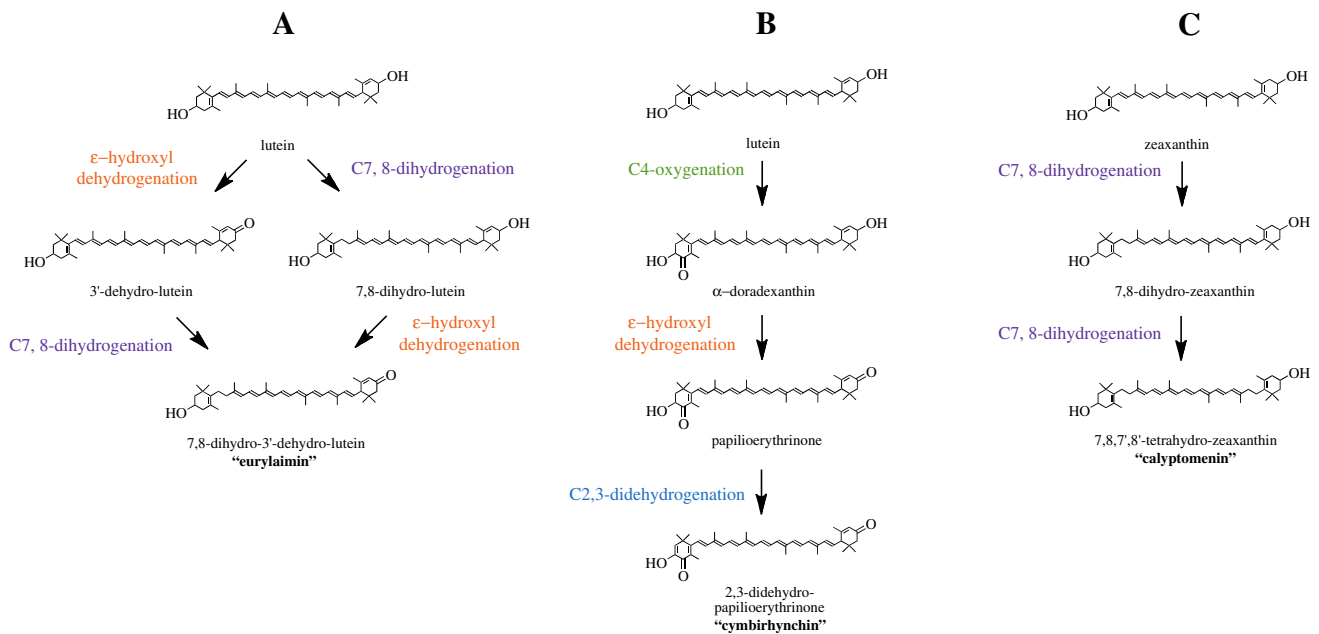


**Fig. 12** Proposed metabolic pathways for the derivation of **a** 7,8-dihydro-3'-dehydro-lutein ("eurylaimin"); **b** 2,3-didehydro-papilioerythrinone ("cymbirhynchin"); and **c** 7,8,7',8'-tetrahydro-zeaxanthin ("calyptomenin"). See text for details

in the production of 7,8-dihydro-xanthophylls in woodpeckers (Stradi et al. 1998; McGraw 2006a). In broadbills, it is uncertain which of these reactions normally proceeds faster, resulting in the two alternative pathways with the production of either 7,8-dihydro-lutein or 3'-dehydro-lutein as intermediates (Fig. 12a). However, the absence of either of the proposed intermediate molecules indicates that both enzymatic reactions occur efficiently enough to convert lutein entirely into eurylaimin (Table 2).

Metabolic production of 2,3-didehydro-papilioerythrinone (cymbirhynchin) likely proceeds from dietary lutein via the intermediates  $\alpha$ -doradexanthin and papilioerythrinone (McGraw 2006a) (Fig. 12b). We hypothesize that papilioerythrinone is produced from lutein via the addition of a carbonyl to C4 in the  $\beta$ -ring and the dehydrogenation of the hydroxyl in the C3' position. Both of these metabolic processes have been previously reported in the formation of 4-ketocarotenoids and canary xanthophylls, respectively (McGraw 2006a; Prager et al. 2009). Then, 2,3-didehydro-papilioerythrinone is likely formed via C2, C3-didehydrogenation (Fig. 11b), a metabolic transformation which we have reported previously in *Xipholena*, *Cotinga*, and other cotingas (LaFountain et al. 2010; Prum et al. 2012a).

The production of 7,8,7',8'-tetrahydro-zeaxanthin (calyptomenin) in *C. viridis* proceeds via the dihydrogenation of the C7, C8 and C7', C8' carbon double bonds of the dietary carotenoid zeaxanthin (Fig. 12c). This reaction has been inferred to occur in woodpeckers (Stradi et al. 1998). Stradi et al. (1998) reported the presence of

7,8,7',8'-tetrahydro-zeaxanthin in three species of woodpeckers: *Picoides villosus*, *Melanerpes candidus*, and *Dryocopus pileatus*. This pigment was always found to occur along with unmodified lutein and in one species (*Picoides villosus*) along with a small concentration of dietary zeaxanthin. They found no evidence of 7,8,7',8'-tetrahydro-lutein in any of the eleven yellow woodpecker plumage patches studied, including *Picus squamatus*, which had near-complete conversion of lutein to 7,8-dihydro-lutein, and *Colaptes melanolaimus* which showed complete conversion to the dihydro-derivative (Stradi et al. 1998). The absence of a tetra-hydrogenated lutein derivative in these two woodpecker species suggests that lutein may not be able to undergo hydrogenation at the C7, C8 bond closest to the  $\epsilon$ -ring. Assuming that there is no physiological mechanism for differential transport of metabolically derived carotenoids into the cells of the feather itself, then if the hydrogenation reaction were able to occur on both C7, C8 and C7', C8' bonds of a lutein molecule, we would expect to observe less of the unmodified lutein precursor in the extract of *Picus squamatus*, and at least some conversion to the tetrahydrogenated lutein derivative (Stradi et al. 1998). Similarly, we would expect to see a significant concentration of tetrahydrogenated lutein derivative in *Colaptes melanolaimus* (Stradi et al. 1998). The absence of unmodified zeaxanthin and presence of a significant amount of unmodified lutein in the plumage of *C. viridis* strongly suggest that, as in woodpeckers, the dihydrogenation of the C7, C8 and C7', C8' carbon double bonds in *C. viridis* is restricted



to the double bonds conjugated with  $\beta$ -rings. We therefore conclude that the tetrahydrogenated molecule calyptomemin is produced exclusively from zeaxanthin.

The pathways that produce the four different, metabolically modified broadbill carotenoids require one to three metabolic reactions each. Broadbills accomplish these different reactions using only four different enzymes, which occur in different combinations in the various pathways (Fig. 12). The evolutionary origins of the enzymes responsible for C4-oxygenation and  $\epsilon$ -hydroxyl-dehydrogenation may have been in the common ancestor of *Cymbirhynchus*, *Eurylaimus*, and *Sarcophanops* (inferred from phylogenies in Irestedt et al. 2006, Moyle et al. 2006). Interestingly, this clade also includes *Serilophus lunatus* which entirely lacks carotenoid feather pigmentation. However, *Serilophus* does have yellow pigmentation of its facial skin and legs that are presumably carotenoids. The C7,8-dihydrogenation enzyme may have evolved independently in the genera *Calyptomena* and *Eurylaimus*, or it may have had a single common ancient origin earlier in the history of the broadbill family.

#### Molecular structure and spectral diversity of broadbill carotenoids

In general, the longer the conjugated chain, the more redshifted the plumage absorbance and reflectance, and the shorter the conjugated chain, the more blueshifted the reflectance. In large part, the conjugation length can explain much of the color variation of carotenoids in the animal kingdom, and the same holds true for broadbills. Indeed, the wavelength of the reflectance slope midpoint for the 7,8-dihydro-xanthophyll plumages of *Eurylaimus* species was exceptionally low at ~475 nm. Similar colors are often found within woodpeckers. This implies that the distinctive light lemon-chiffon yellow appearance of these plumage patches may be a good, visible, and easily measurable indication of a pure 7,8-dihydro-xanthophyll plumage. For example, based on this criterion, we would predict that 7,8-dihydro-xanthophylls will be common in the plumages of New World and Old World barbets (Ramphastidae).

The physiological capacity to alter dietary carotenoids is unusually versatile in the genus *Eurylaimus*. Both *E. javanicus* and *E. ochromalus* can metabolically *lengthen* and *shorten* the conjugated chain of double bonds. This physiological capacity gives rise to the most diverse and divergent carotenoid reflectances found in any single bird plumage: The values of  $\lambda(R_{\text{mid}})$  vary between 475 and 630 nm in the plumage of *E. javanicus*. Previously, only *Colaptes auratus* was known to have the capacity to simultaneously produce 7,8-dihydro-xanthophylls and ketocarotenoids in different plumage patches (Stradi et al. 1998). However, the ketocarotenoids of *Colaptes auratus* are not nearly as redshifted

as the novel papilioerythrinone derivative found in *Eurylaimus*. Thus, the breadth of metabolic capacity to modify carotenoids in *Eurylaimus* produces both distinctive light lemon-yellow and deep lavender purples. *Eurylaimus* species achieve these distinctly colored carotenoid plumage patches by differential deposition of metabolically derived carotenoids into different feathers. It is not known whether these differences are the result of localized metabolic transformation of carotenoids in pigment cells within the developing feather germs, or differential transportation of metabolic products to different areas of the skin.

The capacity to produce diverse carotenoids with short conjugation lengths is shared by broadbills and woodpeckers. Broadbills are in a clade of Old World suboscine perching birds (Eurylaimes, Passeriformes). Woodpeckers are within the zygodactyl Piciformes. Traditionally, the Piciformes were thought to be the closest relatives of the Passeriformes, which could provide some support for the homology of 7,8-dihydro-xanthophyll production within the two families. However, the most recent higher-level phylogenetic analysis of birds places parrots (Psittacidae) as phylogenetically closer to the perching birds (Passeriformes) and places the woodpeckers within a large diverse clade of Piciform–Coraciiform birds (Hackett et al. 2008). Thus, it is more likely that the production of plumage 7,8-dihydro-xanthophylls is convergent between the broadbills and the woodpeckers. Currently, there is little information about the plumage pigments of the many other colorful avian families that are related to broadbills and woodpeckers—including pittas (Pittidae), barbets and toucans (Ramphastidae), bee-eaters (Meropidae), kingfishers (Alcedinidae), etc.

Although the pigment–structure interactions involved in green plumages of *Calyptomena* and *Psarisomus* are outside the scope of the present study, it is interesting to note that *Calyptomena* is the first species known to employ physiologically modified carotenoid pigments—in this case 7,8-dihydro-xanthophylls—in combination with a spongy medullary structural coloration. The result is a distinctively saturated, green structural color. Interestingly, in some populations of *C. viridis*, males have a small dot of yellow feathers on the face in front of the eye that is likely to be a purely carotenoid color (Fig. 2e). This patch was too small to sample during this study.

This study demonstrates that the rather diverse crimson, pink, violet, and purple-maroon plumages of *C. macrorhynchus*, *E. javanicus*, *E. ochromalus*, and *S. steerii* (Fig. 2) are not produced by the same carotenoid pigments as found in plumages of cotingas with similar visible hues. Rather, the ancestor of the *Cymbirhynchus*–*Eurylaimus*–*Sarcophanops* broadbill clade evolved the metabolic capacity to produce a novel ketocarotenoid to create these unusual color effects. Thus, sexual and social selection acting on the plumage

color phenotype in different lineages of birds has resulted in the evolution of independent molecular mechanisms to achieve convergent visual effects. The resulting pigment is derived from papilioerythrinone, which is previously known from male Eurasian Bullfinch (*Pyrrhula pyrrula*), male Gouldian Finch (*Chloebia gouldiae*), and the Pallas' (*Carpodacus roseus*) and Beautiful Rosefinch (*Carpodacus pulcherrimus*) (Stradi et al. 1995a, b, 1997; Stradi 1999; McGraw 2006a). In each of these species, papilioerythrinone occurs with two to five other more commonly known ketocarotenoids, whereas cymbirhynchin constitutes 85–100 % of the carotenoid content of these red broadbill plumages. Furthermore, in none of these other species is the plumage reflectance as redshifted as in these three genera of broadbills. Production of cymbirhynchin from papilioerythrinone requires only one additional metabolic transformation, 2,3-didehydrogenation. Cymbirhynchin produces redshifted plumage reflectance spectra that are equivalent to those recorded for some rhodoxanthin-containing plumages and which approach the reflectance of methoxy-carotenoids of cotingas (e.g., *Phoenicircus*; Prum et al. 2012b). Interestingly, like the pigment 2,3-didehydroxipholenin (i.e., 3'-hydroxy-3-methoxy-2,3-didehydro- $\beta,\epsilon$ -carotene-4-one) identified in the cotinga *Xipholena punicea* (LaFountain et al. 2010), cymbirhynchin has an  $\alpha$ -carotene chromophore with a C4 carbonyl, an adjacent oxygen moiety at C3, and a C2,3 double bond on the  $\beta$ -ring. The two molecules differ in whether  $\beta$ -ring bears a hydroxyl or methoxyl group at C3 and whether C3' of the  $\epsilon$ -ring has a carbonyl or a hydroxyl group.

Several factors may contribute to the extensive variation in color exhibited by feathers with this single ketocarotenoid–cymbirhynchin. These include the following: (1) differences in the concentration of carotenoid; (2) structural coloration; (3) differences in contributions from other pigments (in the present case, phaeomelanins); and (4) genuine shifts in the absorption of the carotenoid itself. Concentration effects could influence the visual appearance. In the present case, the approximately twofold greater concentration of carotenoids in *C. macrorhynchos* could contribute by reducing the blue reflection over the 400–450 nm wavelength range more effectively than in *E. javanicus*. However, saturation effects, which can cause a broadening of the absorption band and therefore shift in the  $\lambda(R_{\text{mid}})$  on the low-energy side, (Hudon et al. 2003) do not appear to play a role because the feather that is more concentrated in carotenoids has the shorter wavelength of  $\lambda(R_{\text{mid}})$ , opposite to expectation. Given the colors involved, structural coloration is unlikely to be a factor in these species. It is possible that a greater concentration of pheomelanins in *C. macrorhynchos* could enhance the blue absorption across the full, observed range from 300 to 550 nm and again lead to a “purer” red reflection, but that is not indicated from the

similar colors of the post-extraction feathers of both species. Finally, both the ~5 nm shift in the  $\lambda(R_{\text{mid}})$  and the ~20 nm difference between the derived absorption spectra are genuine shifts in the absorption bands of the carotenoids, but this shift makes a much smaller contribution to the differences in feather color than do the differences in blue wavelength absorption. Given the relatively small shift in reflectance midpoint, the difference in blue reflectance is the most probable explanation for the color variation from crimson red (*C. macrorhynchos*) to purple-red (*E. javanicus*). Without further study, it is not possible to determine the relative contribution of the carotenoids versus phaeomelanin as the cause of the different reflectance in the blue.

The reflectance spectra of the cymbirhynchin plumage of broadbills are substantially redshifted with respect to standard red, ketocarotenoid plumages of other birds, for example, 581 nm (*Cardinalis cardinalis*, canary xanthophylls, astaxanthin,  $\alpha$ -doradoxanthin, and adonirubin), 583–593 nm (*Euplectes orix*,  $\alpha$ -doradoxanthin and lutein), 575 nm (*Loxia curvirostra*), and 588 nm (*Carpodectes mexicanus* breast, broad sample of ketocarotenoids) (Hudon 1991b; McGraw 2006a; Prager et al. 2009; Stoddard and Prum 2011). The cymbirhynchin plumage reflectance spectra of broadbills are similar in slope midpoint value to the pure rhodoxanthin reflectance of the red-cotingas, e.g., 600–625 nm in *Phoenicircus carnifex* (Prum et al. 2012a), but they do not reach the extreme of the crimson and purple methoxy-carotenoid plumages of cotingas: 660 nm in the purple throat of *Cotinga maynana*, or 667 nm for the maroon crimson belly of *Xipholena punicea* (LaFountain et al. 2010; Prum et al. 2012a). However, some carotenoids with substantially blueshifted absorbance relative to cymbirhynchin have longer conjugated double-bond chain lengths of  $n = 13$  (e.g., astaxanthin, canthaxanthin) or  $n = 14$  (e.g., rhodoxanthin). Therefore, some additional feature of the molecule and its environment is required to explain the redshifted absorption of the crimson-lavender broadbill pigment.

#### Other mechanisms contributing to color variation in broadbill carotenoid plumages

The binding of the ketocarotenoids within a protein can strongly influence the wavelength position of pigment absorption, and this phenomenon is the basis of a wide variety of coloration in animals (Zagalsky 1985, 1995, 2003; Britton et al. 1997). Compared with the absorption maximum of ~460 nm for cymbirhynchin in a largely non-polar solvent, the pigment in feathers has its absorption centered at approximately ~516 nm (*C. macrorhynchos*) or 537 nm (*E. javanicus*). These shifts represent 2,400–3,100  $\text{cm}^{-1}$  of wavelength shift relative to solution that is

caused directly or indirectly by the protein environment. These shifts can be compared with a nearly  $5,000\text{ cm}^{-1}$  redshift seen for astaxanthin in  $\alpha$ -crustacyanin, or the  $\sim 3,700\text{ cm}^{-1}$  redshift in  $\beta$ -crustacyanin (Britton et al. 1997; Zagalsky 2003). The mechanisms by which the environment of the feather can perturb the electronic structure of cymbirhynchin include the following: (1) change in structure (twists of the chromophore, or flattening) (2) polarization (charges or H-bonds) that indirectly affect electron delocalization, as well as the relative energies of the ground and excited states of the chromophore, and (3) exciton coupling between aggregated chromophores. These are addressed below, with emphasis on the rR results.

The rR spectra of cymbirhynchin in the feathers reveal that the chromophores are planar and largely undistorted. To summarize, the  $1,100\text{--}1,400\text{ cm}^{-1}$  fingerprint region is dominated by a single band at  $1,160\text{ cm}^{-1}$  that strongly supports an all-*trans* chromophore. The bands due to HOOP wags have significantly lower intensity than typical spectra of carotenoids in the solution phase. Another indicator of planarity is the primary ethylenic ( $\nu_1$ ) frequency. Although a solution-phase rR spectrum of cymbirhynchin was not acquired, we would expect the frequency to be similar to that of echinenone,  $1,525\text{ cm}^{-1}$  (Salares et al. 1977). The ethylenic frequency of cymbirhynchin within the feathers is lower than this expected frequency by approximately  $6\text{--}9\text{ cm}^{-1}$ . A decrease of  $\sim 5\text{--}10\text{ cm}^{-1}$  is typically observed upon aggregation or crystallization of a carotenoid (Salares et al. 1977; Saito et al. 1983; Wang et al. 2012). One explanation for the downshift is increased planarity of the conjugated backbone (Weesie et al. 1999b; Wang et al. 2012). In summary, the detailed features of the rR spectra of cymbirhynchin within the plumage can be largely rationalized in terms of a relatively flat chromophore.

Although a flat and optimally conjugated chromophore is inferred by vibrational spectroscopy, the  $2,400\text{--}3,100\text{ cm}^{-1}$  bathochromic shifts in the feathers are still unexplained. Unbound carotenoids of various conjugation lengths in solution show a well-established correlation between  $\nu_1$  frequency and the frequency of the absorption maximum, corresponding to a relationship between the extent of conjugation and the difference in energy between ground and excited states (Rimai et al. 1973; Merlin 1987). Specifically, over the limited range of  $\nu_1$  frequencies from  $1,510$  to  $1,530\text{ cm}^{-1}$ , the absorption maximum increases by  $2,400\text{ cm}^{-1}$  in approximately linear fashion, with slope of  $95\text{--}120\text{ cm}^{-1}$  (electronic)/ $1\text{ cm}^{-1}$  (vibrational,  $\nu_1$ ) (Rimai et al. 1973; Merlin 1987; Schaffer et al. 1991). However, the predicted  $20\text{ cm}^{-1}$  downshift in the  $\nu_1$  vibrational frequency is not observed in the rR spectra, indicating that the change in electronic absorption between solution and feather environments cannot be attributed to a change in

conjugation from flattening of the chromophore in the feather.

We now address the second possible influence of feather proteins on the absorption of cymbirhynchin, which is the polarizing influence of charges or H-bonds in the protein matrix that surrounds the carotenoid. These perturbations could affect the delocalization of carotenoid  $\pi$ -electrons and/or the relative energies of the ground and excited states of the chromophore. Given the range of possible interactions, the subject is complex. Other work has interpreted simultaneous shifts in  $\nu_1$  and  $\lambda_{\text{max}}$  as evidence of a polarization mechanism (Salares et al. 1979; Britton et al. 1997). Specifically, the  $\sim 5,000$  or  $3,700\text{ cm}^{-1}$  redshifts in absorption of astaxanthin with  $\alpha$ - or  $\beta$ -crustacyanin, coincident with respective 31 and  $25\text{ cm}^{-1}$  downshifts in  $\nu_1$  frequency, were interpreted as polarization-induced delocalization (Britton et al. 1997; others). By the same measure, one might expect downshifts of 20 or  $26\text{ cm}^{-1}$  for *C. macro-rhynchos* and *E. javanicus*, relative to the chromophore in solution, which are not observed. However, the effect of polarizing charges on absorption and Raman bands in carotenoproteins is still the subject of recent work (Weesie et al. 1999a; van Wijk et al. 2005; Strambi and Durbeej 2009; Neugebauer et al. 2011; Christensson et al. 2013). It must be emphasized that the relatively small downshifts for  $\nu_1$  in our work are not necessarily evidence against a polarization mechanism. In all likelihood, the large  $2,400\text{--}3,100\text{ cm}^{-1}$  shifts in the absorption owe much to the influence of surrounding charged groups and H-bonding. Even if these influences may not have a prominent impact on the rR spectroscopy of the ground state, it is quite likely that changes in dipole moment upon excitation of the asymmetric chromophore are especially large for cymbirhynchin, relative to other carotenoids. The reason is that the chromophore has *two* oxygen groups that are within the conjugated double-bond network, and both are attached to one ring. The third oxygen at the opposite ring is disconnected from the conjugated network. The creation of an enhanced dipole upon excitation would be a mechanism of strong and essentially instantaneous coupling to external charges, which in turn stabilizes the  $S_2$  state relative to a solution environment. The shifts of  $S_2$  caused by external charges are likely large not only because of a large dipole, but also because this state is expected to be more polarizable than the ground state (Krawczyk and Britton 2001).

Finally, we consider the exciton coupling between neighboring, aggregated chromophores, which has also been considered a possible contributor to the redshifted absorption of  $\alpha$ -crustacyanin (Ilagan et al. 2005; van Wijk et al. 2005) as well as in ketocarotenoid feathers (Mendes-Pinto et al. 2012). Exciton coupling is a mechanism by which transition dipoles interact among pigment molecules and alter the excited-state energy levels with little

or no change in the ground state characteristics (Salares et al. 1977; Wang et al. 2012). The small shifts for  $\nu_1$  of cymbirhynchin in feathers, along with the substantial changes in the absorption, are compatible with an exciton coupling mechanism. A bathochromic shift, as observed in this study, would require head-to-tail positions of chromophores (J-type interaction). Pure aggregates of all-*trans* astaxanthin with this kind of geometry appear to be possible and give rise to a redshifted band at 560 nm (Mori et al. 1996). Whether the feather protein matrix is able to enforce the necessary geometry between chromophores in the present work or in prior work where a similar proposal was made (Mendes-Pinto et al. 2012) remains to be seen.

## Conclusions

This work reveals that the brightly colored plumage of Broadbills contain a total of six carotenoid pigments, including two dietary carotenoids, lutein, and zeaxanthin; two rare but previously reported xanthophylls, 7,8-dihydro-zeaxanthin and 7,8,7',8'-tetrahydro-zeaxanthin; and two novel xanthophylls, 7,8-dihydro-3'-dehydro-lutein and 2,3-didehydro-papilioerythrinone. The structure and enol-conformation of 2,3-didehydro-papilioerythrinone were confirmed by NMR spectroscopy. Pathways for all four metabolically derived carotenoids are proposed. The rR spectra strongly suggest that the carotenoid exists in an all-*trans*, planar configuration in situ. Measurements of the reflectance spectra and the absorption lineshapes derived from them revealed a significant redshift of the spectrum of 2,3-didehydro-papilioerythrinone in the feathers of both *C. macrorhynchos* and *E. javanicus* compared to that recorded from the purified pigment in solution. The assessment of the vibrational and electronic spectra in tandem suggests that much of the bathochromic shift of 2,3-didehydro-papilioerythrinone is caused by perturbations that lower the excited-state energy level without significantly perturbing the ground state. The mechanisms could be the polarizing influence of charges nearby the carotenoid, hydrogen bonding, or possibly exciton coupling among neighboring chromophores.

**Acknowledgments** The authors wish to thank Dr. George Britton for helpful discussions. Work in the laboratory of H.A.F. was supported by the University of Connecticut Research Foundation. Work by R.O.P. was supported by the W.R. Coe Fund of Yale University. Work in the laboratory of M.J.T. was supported by the National Science Foundation (under CHE-1057198), and UCSD start-up support. We thank Kristof Zyskowski and the Yale Peabody Museum of Natural History for access to broadbill feather specimens used in this study. We thank Kristof Zyskowski, Bjorn Oleson, and VIREO/Spike Baker for permission to reproduce their photos of broadbills in Fig. 2.

## References

- Bernhard K, Grosjean M (1995) Infrared spectroscopy. In: Britton G, Liaaen-Jensen S, Pfander H (eds) Carotenoids vol 1B: spectroscopy. Birkhäuser Verlag, Basel, pp 117–134
- Britton G (1995) UV/visible spectroscopy. In: Britton G, Liaaen-Jensen S, Pfander H (eds) Carotenoids vol 1B: spectroscopy. Birkhäuser Verlag, Basel, pp 13–62
- Britton G, Weesie RJ, Askin D, Warburton JD, Gallardo-Guerrero L, Jansen FJ, de Groot HJM, Lugtenburg J, Cornard J-P, Merlin J-C (1997) Carotenoid blues: structural studies on carotenoproteins. *Pure Appl Chem* 69:2075–2084
- Britton G, Liaaen-Jensen S, Pfander H (2004) In: Carotenoids handbook. Birkhäuser Verlag, Basel
- Buchecker R, Eugster CH (1979) Eine Suche nach 3'-Epilutein (=3R,3'S,6'R)- $\beta$ ,  $\epsilon$ -Carotin-3,3'-diol) und 3', O-Didehydrolutein (=3R, 6'R)-3-Hydroxy- $\beta$ ,  $\epsilon$ -carotin-3'-on) in Eigelb, in Blüten von *Caltha palustris* und in Herbstblättern. *Helv Chim Acta* 62:2817–2824
- Christensson N, Židek K, Magdaong NCM, LaFountain AM, Frank HA, Zigmantas D (2013) Origin of the bathochromic shift of astaxanthin in lobster protein: 2D electronic spectroscopy investigation of  $\beta$ -crustacyanin. *J Phys Chem B* 117:11209–11219
- Curry B, Palings I, Broek A, Pardo JA, Mulder PPJ, Lugtenburg J et al (1984) Vibrational analysis of 13-cis-retinal. *J Phys Chem* 88:688–702
- Englert G (1995) NMR spectroscopy. In: Britton G, Liaaen-Jensen S, Pfander H (eds) Carotenoids vol 1B spectroscopy. Birkhäuser, Basel, pp 147–259
- Enzell CR, Back S (1995) Mass spectrometry. In: Britton G, Liaaen-Jensen S, Pfander H (eds) Carotenoids vol 1B: spectroscopy. Birkhäuser, Basel, pp 261–317
- Eugster CH (1995) Chemical derivatization: microscale tests for the presence of common functional groups in carotenoids. In: Britton G, Liaaen-Jensen S, Pfander H (eds) Carotenoids vol 1A: isolation and analysis. Birkhäuser Verlag, Basel, pp 71–80
- Eyring G, Curry B, Broek A, Lugtenburg J, Mathies R (1982) Assignment and interpretation of hydrogen out-of-plane vibrations in the resonance Raman spectra of rhodopsin and bathorhodopsin. *Biochemistry* 21:384–393
- Gottlieb HE, Kotlyar V, Nudelman A (1997) NMR chemical shifts of common laboratory solvents as trace impurities. *J Org Chem* 62:7512–7515
- Hackett SJ, Kimball RT, Reddy S, Bowie RCK, Braun EL, Braun MJ et al (2008) A phylogenomic study of birds reveals their evolutionary history. *Science* 320:1763–1768
- Hudon J (1991a) Unusual carotenoid use by the Western Tanager (*Piranga ludoviciana*) and its evolutionary implications. *Can J Zool* 69:2320–23111
- Hudon J (1991b) Unusual carotenoid use by the Western Tanager (*Piranga ludoviciana*) and its evolutionary implications. *Can J Zool* 69:2311–2320
- Hudon J, Grether GF, Millie DF (2003) Marginal differentiation between the sexual and general carotenoid pigmentation of guppies (*Poecilia reticulata*) and a possible visual explanation. *Physiol Biochem Zool* 76:776–790
- Ilagan RP, Christensen RL, Chapp TW, Gibson GN, Pascher T, Polivka T et al (2005) Femtosecond time-resolved absorption spectroscopy of astaxanthin in solution and in  $\alpha$ -crustacyanin. *J Phys Chem A* 109:3120–3127
- Irestedt M, Ohlson JI, Zuccon D, Källersjö M, Ericson PGP (2006) Nuclear DNA from old collections of avian study skins reveals the evolutionary history of the Old World suboscines (Aves, Passeriformes). *Zool J Linn Soc* 150:567–580

- Vetter W, Englert G, Rigassi N, Schwieter U (1971) Spectroscopic methods. In: Isler O (ed) Carotenoids. Birkhäuser Verlag, Basel, pp 189–266
- Koyama Y (1995) Resonance Raman spectroscopy. In: Britton G, Liaaen-Jensen S, Pfander H (eds) Carotenoids vol 1B: spectroscopy. Birkhäuser Verlag, Basel, pp 135–146
- Koyama Y, Fujii R (1999) Cis-trans carotenoids in photosynthesis: configurations, excited-state properties and physiological functions. In: Frank HA, Young AJ, Britton G, Cogdell RJ (eds) The photochemistry of carotenoids, vol 8. Kluwer Academic Publishers, Dordrecht, pp 161–188
- Koyama Y, Hashimoto H (1993) Spectroscopic studies of carotenoids in photosynthetic systems. In: Young AJ, Britton G (eds) Carotenoids in photosynthesis. Chapman and Hall, London, pp 327–408
- Koyama Y, Takatsuka I, Nakata M, Tasumi M (1988) Raman and infrared spectra of the all-trans, 7-cis, 9-cis, 13-cis and 15-cis isomers of *b*-carotene: key bands distinguishing stretched or terminal-bent configurations from central-bent configurations. *J Raman Spectrosc* 19:37–49
- Krawczyk S, Britton G (2001) A study of protein-carotenoid interactions in the astaxanthin-protein crustacyanin by absorption and Stark spectroscopy; evidence for the presence of three spectrally distinct species. *Biochim Biophys Acta* 1544:301–310
- LaFountain AM, Kaligotla S, Cawley S, Riedl KM, Schwartz SJ, Frank HA et al (2010) Novel methoxy-carotenoids from the burgundy-colored plumage of the Pompadour Cotinga *Xipholena punicea*. *Arch Biochem Biophys* 504:142–153
- McGraw KJ (2006a) Mechanics of carotenoid-based coloration. In: Hill GE, McGraw KJ (eds) Bird coloration vol 1: mechanisms and measurements. Harvard University Press, Cambridge, pp 177–242
- McGraw KJ (2006b) Mechanics of melanin-based coloration. In: Hill GE, McGraw KJ (eds) Bird coloration vol 1: mechanisms and measurements. Harvard University Press, Cambridge, pp 243–294
- McGraw KJ, Hill GE, Stradi R, Parker RS (2001) The influence of carotenoid acquisition and utilization on the maintenance of species-typical plumage pigmentation in the male American goldfinches (*Carduelis tristis*) and Northern cardinal (*Cardinalis cardinalis*). *Physiol Biochem Zool* 74:843–852
- McGraw KJ, Hudon J, Hill GE, Parker RS (2005) A simple and inexpensive chemical test for behavioral ecologists to determine the presence of carotenoid pigments in animal tissues. *Behav Ecol Sociobiol* 57:391–397
- Mendes-Pinto MM, LaFountain AM, Stoddard MC, Prum RO, Frank HA, Robert B (2012) Variation in carotenoid-protein interactions by bird feather proteins produces novel plumage coloration. *J R Soc Interface* 9:3338–3350
- Merlin JC (1987) Resonance Raman analysis of astaxanthin-protein complexes. *J Raman Spectrosc* 18:519–523
- Mori Y, Yamano K, Hashimoto H (1996) Bistable aggregate of all-trans-astaxanthin in an aqueous solution. *Chem Phys Lett* 254:84–88
- Moyle RG, Chesser RT, Prum RO, Schikler P, Cracraft J (2006) Phylogeny and evolutionary history of old world suboscine birds (Aves: Eurylaimides). *Am Mus Novit* 3544:1–22
- Neugebauer J, Veldstra J, Buda F (2011) Theoretical spectroscopy of astaxanthin in crustacyanin proteins: absorption, circular dichroism, and nuclear magnetic resonance. *J Phys Chem B* 115:3216–3225
- Prager M, Johansson EIA, Andersson S (2009) Differential ability of carotenoid C4-oxygenation in yellow and red bishop species (*Euplectes* spp.). *Comp Biochem Physiol B* 154:373–380
- Prum RO, LaFountain AM, Berro J, Stoddard MC, Frank HA (2012a) Molecular diversity, metabolic transformation, and evolution of carotenoid feather pigments in cotingas (Aves: Cotingidae). *J Comp Physiol B* 182:1095–1116
- Prum RO, LaFountain AM, Berro J, Stoddard MC, Frank HA (2012b) Molecular diversity, metabolic transformation, and evolution of carotenoid feather pigments in cotingas (Aves: Cotingidae). *J Comp Physiol B* 182:1095–1116
- Rimai L, Heyde ME, Gill D (1973) Vibrational spectra of some carotenoids and related linear polyenes. A Raman spectroscopic study. *J Am Chem Soc* 95:4493–4501
- Robert B (1999) The electronic structure, stereochemistry and resonance Raman spectroscopy of carotenoids. In: Frank HA, Young AJ, Britton G, Cogdell RJ (eds) Advances in photosynthesis, vol 8. Kluwer Academic Publishers, Dordrecht, pp 189–201
- Robert B (2009) Resonance Raman spectroscopy. *Photosynth Res* 101:147–155
- Saito S, Tasumi M, Eugster CH (1983) Resonance Raman-spectra (5800–40 CM<sup>-1</sup>) of all-trans and 15-cis isomers of beta-carotene in the solid-state and in solution-measurements with various laser lines from ultraviolet to red. *J Raman Spectrosc* 14:299–309
- Salares VR, Young NM, Carey PR, Bernstein HJ (1977) Excited state (exciton) interactions in polyene aggregates. *J Raman Spectrosc* 6:282–288
- Salares VR, Young NM, Bernstein HJ, Carey PR (1979) Mechanisms of spectral shifts in lobster carotenoproteins—the resonance Raman spectra of ovoverdin and the crustacyanins. *Biochim Biophys Acta* 576:176–191
- Saranathan V, Forster JD, Noh H, Liew SF, Mochrie SGJ, Cao H et al (2012) Structure and optical function of amorphous photonic nanostructures from avian feather barbs: a comparative small angle X-ray scattering (SAXS) analysis of 229 bird species. *J R Soc Interface* 9:2563–2580
- Schaffer HE, Chance RR, Silbey RJ, Knoll K, Schrock RR (1991) Conjugation length dependence of Raman scattering in a series of linear polyenes: implications for polyacetylene. *J Chem Phys* 94:4161–4170
- Schiedt K, Liaaen-Jensen S (1995) Isolation and analysis. In: Britton G, Liaaen-Jensen S, Pfander H (eds) Carotenoids vol 1A: isolation and analysis. Birkhäuser Verlag, Basel, pp 81–107
- Stoddard MC, Prum RO (2011) How colorful are birds? Evolution of the avian plumage color gamut. *Behav Ecol* 22:1042–1052
- Stradi R (1999) Pigmenti e sistematica degli uccelli. In: Brambilla L, Canali G, Mannucci E, Massa R, Saino N, Stradi R, Zerbi G (eds) Colori in volo: il piumaggio degli uccelli. Università degli Studi di Milano, Milan, pp 117–146
- Stradi R, Celentano G, Nava D (1995a) Separation and identification of carotenoids in bird's plumage by high-performance liquid chromatography-diode-array detection. *J Chromatogr B* 670:337–348
- Stradi R, Celentano G, Rossi E, Rovati G, Pastore M (1995b) Carotenoids in bird plumage: the carotenoid pattern in a series of Palearctic *Carduelinae*. *Comp Biochem Physiol* 110B:131–143
- Stradi R, Rossi E, Celentano G, Bellardi B (1996) Carotenoids in bird plumage: the pattern in three *Loxia* species and in *Pinicola enucleator*. *Comp Biochem Physiol* 113B:427–432
- Stradi R, Celentano G, Boles M, Mercato F (1997) Carotenoids in bird plumage: the pattern in a series of red-pigmented *Carduelinae*. *Comp Biochem Physiol* 117B:85–91
- Stradi R, Hudon J, Celentano G, Pini E (1998) Carotenoids in bird plumage: the complement of yellow and red pigments in true woodpeckers (*Picinae*). *Comp Biochem Physiol B: Biochem Mol Biol* 120:223–230
- Strambi A, Durbeej B (2009) Excited-state modeling of the astaxanthin dimer predicts a minor contribution from exciton coupling to the bathochromic shift in crustacyanin. *J Phys Chem B* 113:5311–5317

- van Breemen RB, Dong L, Pajkovic ND (2012) Atmospheric pressure chemical ionization tandem mass spectrometry of carotenoids. *Int J Mass Spectrom* 312:163–172
- van Wijk AA, Spaans A, Uzunbajakava N, Otto C, de Groot HJ, Lugtenberg J et al (2005) Spectroscopy and quantum chemical modeling reveal a predominant contribution of excitonic interactions to the bathochromic shift in alpha-crustacyanin, the blue carotenoprotein in the carapace of the lobster *Homarus gammarus*. *J Am Chem Soc* 127:1438–1445
- Veronelli M, Zerbi G, Stradi R (1995) In-situ resonance Raman-spectra of carotenoids in birds feathers. *J Raman Spectrosc* 26:683–692
- Wang C, Berg CJ, Hsu C-C, Merrill BA, Tauber MJ (2012) Characterization of carotenoid aggregates by steady-state optical spectroscopy. *J Phys Chem B* 116:10617–10630
- Weesie RJ, Merlin JC, De Groot HJM, Britton G, Lugtenberg J, Jansen FJ et al (1999a) Resonance Raman spectroscopy and quantum chemical modeling studies of protein-astaxanthin interactions in a-crustacyanin (major blue carotenoprotein complex in carapace of lobster, *Homarus gammarus*). *Biospectroscopy* 5:358–370
- Weesie RJ, Merlin JC, Lugtenberg J, Britton G, Jansen FJ, Cornard JP (1999b) Semiempirical and Raman spectroscopic studies of carotenoids. *Biospectroscopy* 5:19–33
- Zagalsky PF (1985) Invertebrate carotenoproteins. In: Law JH, Rilling HC (eds) *Methods in enzymology*, vol III: steroids and isoprenoids part B. Academic Press, New York, pp 216–247
- Zagalsky PF (1995) Carotenoproteins. In: Britton G, Liaaen-Jensen S, Pfander H (eds) *Carotenoids*, vol 1A. Birkhauser, Basel, pp 287–294
- Zagalsky PF (2003)  $\beta$ -Crustacyanin, the blue-purple carotenoprotein of lobster carapace: consideration of the bathochromic shift of the protein-bound astaxanthin. *Acta Crystallogr D* 59:1529–1531